Publications of the Astronomical Society of the Pacific, 132:101001 (19pp), 2020 October https://doi.org/10.1088/1538-3873/aba6a0

Exocomets from a Solar System Perspective

Paul A. Strøm[1], Dennis Bodewits[2], Matthew M. Knight[3,4], Flavien Kiefer[5], Geraint H. Jones[6,7], Quentin Kral[8], Luca Matrà[9], Eva Bodman[10], Maria Teresa Capria[11], Ilsedore Cleeves[12], Alan Fitzsimmons[13], Nader Haghighipour[14], John H. D. Harrison[15], Daniela Iglesias[16], Mihkel Kama[17,18], Harold Linnartz[19], Liton Majumdar[20], Ernst J. W. de Mooij[13], Stefanie N. Milam[21], Cyrielle Opitom[22,23], Isabel Rebollido[24], Laura K. Rogers[15], Colin Snodgrass[23], Clara Sousa-Silva[25], Siyi Xu (许偲艺)[26], Zhong-Yi Lin[27], and Sebastian Zieba[28,29]

[1] Department of Physics, University of Warwick, Coventry CV4 7AL, UK; paul.a.wilson@warwick.ac.uk
[2] Department of Physics, Auburn University, Leach Science Center, Auburn, AL 36832, USA
[3] Department of Physics, United States Naval Academy, 572C Holloway Rd, Annapolis, MD 21402, USA
[4] Department of Astronomy, University of Maryland, College Park, MD 20742, USA
[5] Sorbonne Université, CNRS, UMR 7095, Institut d'Astrophysique de Paris, 98 bis bd Arago, F-75014 Paris, France
[6] Mullard Space Science Laboratory, University College London, Holmbury St. Mary, Dorking, Surrey RH5 6NT, UK
[7] The Centre for Planetary Sciences at UCL/Birkbeck, London, UK
[8] LESIA, Observatoire de Paris, Université PSL, CNRS, Sorbonne Université, Université de Paris, 5 place Jules Janssen, F-92195 Meudon, France
[9] School of Physics, National University of Ireland Galway, University Road, Galway, Ireland
[10] School of Earth and Space Exploration, Arizona State University, P.O. Box 871404, Tempe, AZ 85287-1404, USA
[11] Istituto di Astrofisica e Planetologia Spaziali (IAPS), INAF, via del Fosso del Cavaliere, I-00133 Roma, Italy
[12] University of Virginia, Charlottesville, VA 22904, USA
[13] Astrophysics Research Centre, School of Mathematics and Physics, Queen's University Belfast, Belfast, UK
[14] Institute for Astronomy, University of Hawaii-Manoa, Honolulu, HI 96825, USA
[15] Institute of Astronomy, University of Cambridge, Madingley Road, Cambridge CB3 0HA, UK
[16] Instituto de Física y Astronomía, Facultad de Ciencias, and Núcleo Milenio de Formación Planetaria—NPF, Universidad de Valparaíso, Av. Gran Bretaña 1111, 5030 Casilla, Valparaíso, Chile
[17] Tartu Observatory, Observatooriumi 1, Tõravere 61602, Tartumaa, Estonia
[18] Department of Physics and Astronomy, University College London, Gower Street, London, WC1E 6BT, UK
[19] Laboratory for Astrophysics, Leiden Observatory, PO Box 9513, NL2300 RA Leiden, The Netherlands
[20] School of Earth and Planetary Sciences, National Institute of Science Education and Research, HBNI, Jatni 752050, Odisha, India
[21] NASA Goddard Space Flight Center, Astrochemistry Laboratory, Code 691, Greenbelt, MD 20771, USA
[22] ESO (European Southern Observatory), Alonso de Cordova 3107, Vitacura, Santiago, Chile
[23] Institute for Astronomy, University of Edinburgh, Royal Observatory, Edinburgh EH9 3HJ, UK
[24] Departamento de Física Teórica, Universidad Autónoma de Madrid, Cantoblanco, E-28049 Madrid, Spain
[25] Earth, Atmospheric, and Planetary Sciences Department, Massachusetts Institute of Technology, Cambridge, MA 02139, USA
[26] NSF's NOIRLab/Gemini Observatory, 670 N'ohoku Place, Hilo, HI 96720, USA
[27] Institute of Astronomy, National Central University, Chung-Li 32054, Taiwan
[28] Max-Planck-Institut für Astronomie, Königstuhl 17, D-69117 Heidelberg, Germany
[29] Leiden Observatory, Leiden University, PO Box 9513, 2300 RA Leiden, The Netherlands
Received 2020 April 23; accepted 2020 July 16; published 2020 September 16

Abstract

Exocomets are small bodies releasing gas and dust which orbit stars other than the Sun. Their existence was first inferred from the detection of variable absorption features in stellar spectra in the late 1980s using spectroscopy. More recently, they have been detected through photometric transits from space, and through far-IR/mm gas emission within debris disks. As (exo)comets are considered to contain the most pristine material accessible in stellar systems, they hold the potential to give us information about early stage formation and evolution conditions of extra solar systems. In the solar system, comets carry the physical and chemical memory of the protoplanetary disk environment where they formed, providing relevant information on processes in the primordial solar nebula. The aim of this paper is to compare essential compositional properties between solar system comets and exocomets to allow for the development of new observational methods and techniques. The paper aims to highlight commonalities and to discuss differences which may aid the communication between the involved research communities and perhaps also avoid misconceptions. The compositional properties of solar system comets and exocomets are summarized before providing an observational comparison between them. Exocomets likely vary in their composition depending on their formation environment like solar system comets do, and since exocomets are not resolved spatially, they pose a challenge when comparing them to high fidelity observations

of solar system comets. Observations of gas around main sequence stars, spectroscopic observations of "polluted" white dwarf atmospheres and spectroscopic observations of transiting exocomets suggest that exocomets may show compositional similarities with solar system comets. The recent interstellar visitor 2I/Borisov showed gas, dust and nuclear properties similar to that of solar system comets. This raises the tantalising prospect that observations of interstellar comets may help bridge the fields of exocomet and solar system comets.

Key words: Comets – Kuiper belt – Main-belt comets – Photometry – Small solar system bodies – Spectroscopy

Online material: color figures

1. Introduction

Solar system comets are small bodies containing volatiles which sublimate on close approach to the Sun, creating a cloud of dust and gas. Together with asteroids they are regarded as the unused building blocks of the solar system and much is to be gained by studying their composition and evolution as they provide important clues to the formation of the solar system (A'Hearn 2017; Eistrup et al. 2019). The accretion of icy solids including comets is a widely accepted formation scenario for the cores of the giant planets (e.g., Lissauer 1993; Pollack et al. 1996; Lambrechts & Johansen 2014; Bitsch et al. 2015, 2019; Alibert et al. 2018). At a later stage of planet formation comets may have contributed to the delivery of water likely enriched with complex organic molecules to the terrestrial planets in the solar system, although it is still argued whether or not the comets dominate that later delivery (Hartogh et al. 2011; Altwegg et al. 2015; Jin & Bose 2019; Lis et al. 2019).

The comparison between small bodies in the solar system with those around other stars provides a unique window on planet formation processes that can ultimately help us address questions regarding planet formation, and early complex chemistry. The first unambiguously active interstellar exocomet to pass through the solar system was recently detected and characterized (Fitzsimmons et al. 2019; Guzik et al. 2019; Opitom et al. 2019a). The exocomet, known as 2I/Borisov, showed gas, dust and nuclear properties similar to that of solar system comets, but was enriched in CO (Bodewits et al. 2020; Cordiner et al. 2020).

The presence of sublimating small bodies orbiting other stars, commonly referred to as "exocomets," has been inferred ever since variable absorption features were detected in the Ca II lines of the star β Pictoris (β Pic) by Ferlet et al. (1987). The term "Falling Evaporating Bodies" (FEBs) has been used interchangeably with exocomets since Beust et al. (1990). There are four stellar systems with observations showing variable exocomet absorption signatures in several lines or which exhibit a clear photometric signature which is attributed to exocomet activity (see Table 1). There are an additional ~30 systems which show variability in one of the Ca II H or K lines or weak photometric signatures that are suggestive of exocomets (see Table 2). Recent advances in space based photometers such as the Kepler Space Telescope and the Transiting Exoplanet Survey Satellite (TESS) have enabled the photometric detections of exocomets as they transit their host star (Kiefer et al. 2017; Rappaport et al. 2018; Kennedy et al. 2019; Zieba et al. 2019) which accurately match predictions on the transit shape and depth (Lecavelier Des Etangs 1999; Lecavelier Des Etangs et al. 1999). Minute irregular dips in stellar light curves have been interpreted as transits of swarms of exocomets (e.g., Wyatt et al. 2018). A large fraction of main sequence stars with cold planetesimal belts exhibit traces of gas (e.g., Marino et al. 2016; Kral et al. 2017b; Moór et al. 2017; Matrà et al. 2019a), interpreted as being released by volatile-rich minor bodies (Zuckerman & Song 2012; Kral et al. 2016).

The "pollution" of white dwarf (WD) atmospheres has been attributed to the accretion of large extrasolar minor bodies with masses (10^{16}–10^{23} kg) equivalent to solar system asteroids (Farihi et al. 2010; Girven et al. 2012; Veras 2016). Detailed abundance studies (e.g., Jura 2006; Xu et al. 2013; Harrison et al. 2018) suggest that in the majority of the studied systems the accreting material is volatile-poor and rocky, thus, the material is compositionally similar to solar system asteroids. However, Xu et al. (2017) found evidence for the accretion of volatile-rich icy material in the WD1425+540 system. The photospheric C, N, and O abundances of WD1425+540 relative to the photospheric refractory abundances (Mg, Si, Fe etc.) were not only consistent with icy material (Harrison et al. 2018) they also resembled the composition of the solar system comet 1P/Halley. This suggests that polluted WDs could be useful probes of the bulk composition of exocomets.

Despite the great opportunity for exocometary scientists and the solar system comet community to learn from each other and exchange experiences and techniques, there has been surprisingly little collaboration between them. This paper is the product of a workshop at the Lorentz Centre in Leiden, the Netherlands, in 2019 May, which brought experts from these communities together in the same room to share ideas and exchange knowledge and to foster new insights and develop fresh approaches to a very timely topic. As such, this paper is not meant as a comprehensive review of the different fields. Rather, it should serve as an introduction to some core discoveries, provide access to standard and useful references, identify open issues in both fields, and point out common misconceptions. In Section 2, we summarize some key properties of comets in the solar system. Then in Section 3, we provide a brief overview of the properties of exocomets. In Section 4, we compare the observational similarities and differences between solar system comets and exocomets before

Table 1
Stars with Observations Showing Spectral or Photometric Variability Conclusively Attributed to Exocomet Activity

Name	Sp. Type	References
49 Cet (HD 9672)	A1V	(1)
β Pic (HD 39060)	A6V	(2), (3)
HD 172555	A7V	(4)
KIC 3542116 (Photometric detection)	F2V	(5)

References. (1) Montgomery & Welsh (2012), (2) Ferlet et al. (1987), (3) Kiefer et al. (2014b), (4) Kiefer et al. (2014a), (5) (Rappaport et al. 2018). Spectral types were taken from the references.

Table 2
Stars Which Show Variability in One of the Ca II H or K Lines or Weak Photometric Signatures that are Suggestive of Exocomet Activity

Name	Sp. Type	Reference
HD 256 (HR 10)[a]	A2IV/V	(1), (12), (15), (20), (28)
HD 21620	A0V	(3)
HD 32297	A0V	(4)
HD 37306 (HR 1919)	A1V	(29)
HD 42111	A3V	(5), (12)
HD 50241	A7IV	(5), (11)
HD 56537 (λ Gem)	A3V	(6)
HD 58647	B9IV	(6)
HD 64145 (ϕ Gem)	A3V	(6)
HD 80007 (HR 3685)	A2IV	(11), (15)
HD 85905	A2V	(7), (15)
HD 98058 (ϕ Leo)	A5V	(30)
HD 108767 (δ Crv)	A0IV	(6)
HD 109573 (HR 4796)	A0V	(6), (16)
HD 110411 (ρ Vir)	A0V	(3)
HD 138629 (HR 5774)	A5V	(8)
HD 132200 (κ Cen)	B2IV	(19)
HD 145964	B9V	(3)
HD 148283 (HR 6123)	A5V	(5), (13)
HD 156623 (HIP 84881)	A0V	(19)
HD 182919 (5 Vul)	A0V	(2)
HD 183324 (c Aql)	A0IV	(10), (16)
HD 217782 (2 And)	A3V	(2), (5), (14)
HD 24966	A0V	(21)
HD 38056	B9.5V	(21)
HD 79469 (θ Hya)	B9.5V	(21)
HD 225200	A1V	(21)
KIC 11084727 (Phot.)	F2V	(22)
KIC 8462852 (Phot.)	F3V	(23), (24), (25), (26), (27)

Note.
[a] The star HD 256 (HR 10), while reported in the literature repeatedly as an exocomet-host star, is also a binary with both components hosting a circumstellar stable component (see Montesinos et al. 2019). We present the object in this table to showcase that care must be taken to verify potential false positives and because there still remains unexplained weaker absorptions seen in high resolution spectroscopy by Welsh et al. (1998) which may not correspond to the signatures reported in Montesinos et al. (2019).

References. (1) Lagrange-Henri et al. (1990a), (2) Montgomery & Welsh (2012), (3) Welsh & Montgomery (2013), (4) Redfield (2007), (5) Roberge & Weinberger (2008), (6) Welsh & Montgomery (2015), (7) Welsh et al. (1998), (8) Lagrange-Henri et al. (1990b), (9) Kiefer et al. (2014a), (10) Montgomery & Welsh (2017), (11) Hempel & Schmitt (2003), (12) Lecavelier Des Etangs et al. (1997a), (13) Grady et al. (1996), (14) Cheng & Neff (2003), (15) Redfield et al. (2007), (16) Iglesias et al. (2018), (17) Ferlet et al. (1987), (18) Kiefer et al. (2014b), (19) Rebollido et al. (2018), (20) Eiroa et al. (2016), (21) Welsh & Montgomery (2018) (22) Rappaport et al. (2018), (23) Boyajian et al. (2016), (24) Bodman & Quillen (2016), (25) Kiefer et al. (2017), (26) Deeg et al. (2018), (27) Wyatt et al. (2018), (28) Montesinos et al. (2019), (29) Iglesias et al. (2019), (30) Eiroa et al. (2016). Spectral types were taken from the references.

briefly discussing the discovery of interstellar visitors in Section 5. Finally we provide a summary and an outlook in Section 6.

2. Properties of Comets in the Solar System

2.1. Ice Content and Sublimation

For comets, "activity" usually refers to the sublimation of ices stored in the nucleus. The expanding gas drags small dust (and sometimes ice) particles along. The main ices in most comet nuclei are H_2O, CO_2, and CO; their relative abundances appear to vary greatly among comets and may be a primordial property (A'Hearn et al. 2012; Ootsubo et al. 2012; Bockelée-Morvan & Biver 2017).

These ices have very different sublimation temperatures and can therefore start to effectively sublimate at different distances from the Sun (Meech & Svoren 2004; Burke & Brown 2010). The onset of significant effective sublimation of H_2O ice from the comet nucleus occurs at 180 K or 2.5 au from the Sun; CO_2 at 80 K or out to 13 au; and CO at 25 K or 120 au. It is of note that sublimation does not stop outside these distances but rates drop off exponentially. Consequently, comets can be active at great distances from the Sun (Jewitt et al. 2019).

Typical water sublimation rates of comets observed from Earth are between 10^{27} and 10^{30} water molecules s^{-1}, equivalent to 30–30,000 kg s^{-1}. Jupiter Family comets typically reach water production rates of order 10^{28} molecules s^{-1}; whereas Oort Cloud comets frequently reach 10^{29} molecules s^{-1}. Sustained comet water production rates above a level of $\sim 5 \times 10^{29}$ molecules s^{-1} are exceptional (A'Hearn et al. 1995). The largest reported are for comets C/1975 V1 (West) and C/1995 (Hale–Bopp), which both reached peak water production rates above 10^{31} molecules s^{-1} (A'Hearn et al. 1995; Biver et al. 1997), though higher production rates likely briefly occur in the case of comets that get extremely close to the Sun. For example, C/2011 W3 (Lovejoy) had production rates $\sim 10^{31}$ molecules s^{-1} despite having a nucleus that was at least an order of magnitude smaller than that of Hale–Bopp (Raymond et al. 2018a).

The Rosetta spacecraft traveled alongside comet 67P/Churyumov–Gerasimenko for two years and found that the percentage of surface that can be considered as "active" varies greatly along the orbit, and is influenced not only by the illumination geometry but also by local structural and compositional properties (Combi et al. 2020). For most comets, only a small fraction of the surface, of order 5%, contributes to the sublimation activity (A'Hearn et al. 1995), but there are

comets for which significantly more of the surface appears to be active (Bodewits et al. 2014). Other comets eject large amounts of icy grains that seemingly exaggerate the nucleus's active surface area (such as 103P/Hartley 2; A'Hearn et al. 2011).

Comet-like, sublimation-driven activity can occur even if an object contains no water ice. Silicates will start to sublimate at 1000–1500 K, depending on their Mg/Fe content (see Figure 17 in Jones et al. 2018). Such temperatures occur only when objects get within ∼0.1 au of the Sun. Asteroid (3200) Phaethon has displayed faint comet-like activity near its perihelion at 0.14 au, with a variety of mechanisms suggested for this behavior (Jewitt & Li 2010).

Very little is known about comet interiors and how ices are stored and mixed within them (A'Hearn 2017). The dust-to-ice ratio of comets is an area of active debate; the Rosetta mission to comet 67P/Churyumov–Gerasimenko suggested that its nucleus may contain far less volatile material than was previously assumed for comets, with a refractory to ice ratio of 6 ± 3 in this object (Fulle et al. 2017, 2019; Choukroun et al. 2020). In addition, it is a long-standing question whether comets (and other small bodies such as Centaurs) contain amorphous water ice, whose conversion to crystalline ice could drive activity at large distances from the Sun (Prialnik & Bar-Nun 1987; Meech & Svoren 2004; Guilbert-Lepoutre 2012; Agarwal et al. 2017).

Once ejected material has left the vicinity of a solar system comet's nucleus, it forms the comet's dust and ion tails. Neutral cometary gas is ionized by photoionization, charge transfer with solar wind protons, and electron impact ionization (Cravens 1991). Solar system comets are immersed in the solar wind, a continuous anti-sunward stream of ionized material flowing at several hundred km per second. Once ionized, this plasma is subsumed by the solar wind, forming an ion tail which can be observed remotely. Ion tails can span several astronomical units in length and often appear blue due to the resonant fluorescent emission of CO^+ (next section). Cometary dust is accelerated anti-sunward by radiation pressure, generally following the classic dust tail formation process first formulated by Finson & Probstein (1968). There are indications that dust can also be affected by the solar wind, i.e., that it is electrically charged, and is affected by the plasma flowing from the Sun, e.g., Kramer et al. (2014), Price et al. (2019).

2.2. Chemical and Elemental Composition of the Gas and Dust

Most of our knowledge about the composition of comets comes from observations of the gas and dust surrounding them. The elemental composition of comet dust has been studied in situ by instruments on board spacecraft like Vega 1 and 2, Giotto, and Rosetta (Cochran et al. 2015; Bardyn et al. 2017), in laboratories on Earth by collecting particles in Earth's upper atmosphere (Sykes et al. 2004), and directly from a comet's atmosphere by the Stardust mission (Brownlee 2014). The Giotto, Stardust, and Rosetta–COSIMA results were consistent and showed that approximately 50% of the mass of the cometary dust is solid organic matter (the other half consisting of minerals) and that the average elemental composition is close to that of the Sun (Bardyn et al. 2017) with H and He being notable exceptions (they are more abundant in the Sun). Remote observations of dust are most diagnostic in the mid-infrared, where there are absorption features of minerals, but this has only been possible for relatively few bright comets (Wooden et al. 2017). In optical and near-IR wavelengths, the spectrum of comet dust is mostly featureless and slightly reddened with respect to sunlight. There is a very strong forward scattering phase effect (e.g., Marcus 2007; Bertini et al. 2017) that can enhance the dust's brightness by a factor 1000 or more at phase angles above 175° (Hui 2013).

Most remote gas-phase chemical abundances are measured with respect to H_2O. At distances further than 2.5 au from the Sun, the sublimation rates of water decline quickly. The relative abundance at larger heliocentric distances thus does not represent the ice composition of the nucleus (Ootsubo et al. 2012). After H_2O, the main components of gas comae are usually CO and CO_2 (both 0%–30% with respect to H_2O; A'Hearn et al. 2012). Additionally, smaller amounts of other molecules are routinely observed in active comets, including CH_4, HCN, CH_3OH, H_2S, etc. Inventories of molecules are given in dedicated review papers (Mumma & Charnley 2011; Bockelée-Morvan & Biver 2017; Altwegg & ROSINA Team 2018; Altwegg et al. 2019). The ROSINA instrument on board Rosetta detected more than 55 different species surrounding 67P/Churyumov–Gerasimenko (Altwegg & ROSINA Team 2018), including the amino acid glycine (Altwegg et al. 2016), molecular oxygen (Bieler et al. 2015), and the noble gases Ar and Xe (Balsiger et al. 2015; Marty et al. 2017).

Finally, there are many ions, radicals, and fragment species that are formed by physical reactions in the coma or as products of photodissociation, such as CO^+, H_2O^+, CN, CS, OH, C_3, C_2 etc. (A'Hearn et al. 1995; Fink 2009; Cochran et al. 2012). Many of these species have been observed from the ground in numerous comets because they have relatively large fluorescence efficiencies, are often longer lived than their parents, and they are accessible at multiple wavelengths and with different techniques. However, the origin of many fragment species is unknown or ambiguous (Feldman et al. 2004). An often encountered question in cometary volatiles is therefore whether they are native to the comet nucleus or formed from other processes on the surface or in the coma.

2.3. Spectroscopic Features of Comets

Cometary contents have been studied and detected in almost every part of the electromagnetic spectrum (see Table A1 for a summary of features). In this section, we aim to identify the brightest and most useful features, the processes that drive

them, and some of the diagnostics they provide. We recall here that this paper is intended as a broad overview which applies to remote observations of comets, typically at a distance of 1 au from Earth and the Sun. On a one-by-one case, comets can behave very differently, caused by, for example, different observing circumstances (extremely close approaches to Earth, space missions), or intrinsic physical properties (very low or high production rates, close proximity to the Sun, unusual chemical composition). Given the depth and long history of comet science, this work is also not intended as an exhaustive review, but merely to provide some useful starting points and examples. There are a number of reviews that provide a more comprehensive overview of the field (including Feldman et al. 2004; Mumma & Charnley 2011; Cochran et al. 2015; Bockelée-Morvan & Biver 2017).

Gases in the coma of solar system comets emit light throughout the electromagnetic spectrum through different excitation mechanisms. At most wavelengths, the dominant process observed is solar pumped fluorescence where small molecules re-emit upon excitation with high efficiency. A second process is emissive photodissociation, also known as prompt emission, where photodissociation produces excited fragments ([O I], [N I], [C I]; see McKay et al. 2013; Opitom et al. 2019b). Third, in the inner coma, electron impact dissociation reactions may produce excited atomic and molecular fragments such as H, [O I], CO, OH, etc. (Feldman et al. 2015; Bodewits et al. 2016). Given the right conditions this emission mechanism can reveal small traces of volatiles. In a different setting it also led to the discovery of H_2O plumes above the surface of Europa (Roth et al. 2014).

In 1996, Chandra and the Extreme UltraViolet Explorer unexpectedly discovered that comets can be bright (>1 GW) extreme ultraviolet and X-ray sources (Lisse et al. 1996; Krasnopolsky et al. 1997). When highly charged solar wind ions (O^{8+}, O^{7+}, C^{6+}, ...) collide with the neutral gas surrounding comets, the ions capture one or more electrons into an excited state. As they cascade to the ground state, they emit X-rays (Cravens 1997). This charge exchange emission has distinct spectral features different from thermally excited plasmas and can be used to help characterize the solar wind plasma and structures such as comets' solar wind bow shocks (Wegmann et al. 2004), the amount of neutral gas present, and possibly even its composition (Bodewits et al. 2007; Mullen et al. 2017).

In the far- and mid-ultraviolet (120–300 nm), several bright emission lines from atoms such as H, C, and O can be detected. The fluorescent Lyα emission of atomic hydrogen is routinely used to determine comet water production with the Solar Wind Anisotropies/Solar and Heliospheric Observatory (SWAN/SOHO) survey instrument (see Combi et al. 2011). Notable other bright emission features are the CO fourth positive system (130–190 nm; Lupu et al. 2007), the forbidden Cameron bands of CO (190–280 nm; Weaver et al. 1994), and the CO_2^+ feature around 289 nm (Festou 1981).

At near-UV and optical wavelengths (300–700 nm), the most commonly observed lines are from fragment species (OH, CN, C_2, etc.), which emit at easily accessible optical wavelengths and have very high fluorescence efficiencies. Several high-quality line atlases are available for optical spectra (including Cochran & Cochran 2002; Cremonese et al. 2002, and Brown et al. 1996). Comet-specific narrowband filters (Farnham et al. 2000; Schleicher & Farnham 2004) are commonly used to image the distribution of fragment species in the coma and to survey production and mixing rates (A'Hearn et al. 1995).

The strongest feature in this region is the OH A $^2\Sigma^+$–X $^2\Pi_i$ (0-0) band around 308.5 nm but due to significant atmospheric extinction in the near-UV and limited telescope facilities that are sufficiently blue sensitive, it is often challenging to study. Instead, the strong CN B $^2\Sigma^+$–X $^2\Sigma^+$ violet band near 388.3 nm is generally the most accessible bright cometary feature (see Feldman et al. 2004) that was already identified 139 yr ago (Huggins 1881). Although the chemical source of CN is debated (several comets have more CN than its presumed parent HCN), its emission has been detected at large distances (>5 au) from the Sun, e.g., Cochran & Cochran (1991), Schleicher et al. (1997). Another feature that can be very bright is the CO^+ A $^2\Pi$–X $^2\Sigma$ "comet tail" emission between 300 and 500 nm (see Opitom et al. 2019b), although the brightness of this feature tends to vary substantially between comets, presumably due to the wide range of involved CO abundances (Dello Russo et al. 2016). Also small carbon chain radicals have been observed. In the 19th century, Huggins (1881) observed a blue band at 405.2 nm in the spectrum of comet Tebbutt, that later was identified as arising from C_3 emission (Douglas 1951).

Emission from neutral Na may also be seen in solar system cometary spectra, particularly those of near-Sun comets (Jones et al. 2018 and references therein). The origin of this species in these comets is undetermined. Occasionally, spectra have Na features at two distinct velocities (Cremonese 1999; Leblanc et al. 2008), possibly suggesting multiple sources. The Rosetta spacecraft did detect Na in dust grains (Schulz et al. 2015), but a consensus on a dust and/or nuclear ice source in different comets has not yet been reached (e.g., see Cremonese 1999 and Cremonese et al. 2002 for reviews). Ellinger et al. (2015) have suggested an ice source of Na. Sodium observations are discussed further in Section 4.3. Despite being key species in exocomet studies, the Ca^+ ion, and the neutral Ca species, have been observed in a few solar system comets, with the bright sungrazer C/1965 (Ikeya–Seki) being the first where Ca I and Ca II were detected remotely in significant abundances (Slaughter 1969). Their sources are undetermined.

Parent molecules are generally observed at infrared, submillimeter, and millimeter wavelengths (Bockelée-Morvan et al. 2004; Mumma & Charnley 2011; Cordiner et al. 2014). Symmetric species lacking permanent dipoles and therefore pure rotational spectra (CO_2, CH_4, C_2H_2, C_2H_6, C_2H_4,…) can

only be observed through rovibrational transitions in the IR upon asymmetric excitations, while other polar complex volatiles excited by solar radiation and/or collision processes, also exhibit pure rotational transitions at radio wavelengths. Measurements at these wavelengths offer insight into the molecular complexity of cometary comae (Biver et al. 2015), distribution of species throughout the comae (Cordiner et al. 2014), as well as other physical mechanisms such as jet activity, rotation, gas temperature profile, distributed sources, etc. (see Drahus et al. 2010; Bonev et al. 2013; Cordiner et al. 2017). These techniques are entering a new era in sensitivity, resolution, and bandwidth (allowing the coverage of multiple molecules simultaneously) that will not only significantly advance comet studies within the solar system, but likely also be employed for future studies of exocomets.

As is the case with other astronomical spectroscopic fields, the complete and accurate interpretation of cometary composition is limited by the availability of high-quality spectral data, such as comprehensive line lists and accurate broadening parameters. Currently, complete spectral data only exists for a fraction of the molecular species that could be present in comets (Sousa-Silva et al. 2019). As such, cometary spectra are vulnerable to misinterpretation, and molecular detections susceptible to misassignments. Table A1 highlights the complexity of molecular composition of comet spectra, with dozens of molecular species already discovered. It is therefore plausible that many more molecules are present in comets that cannot yet be correctly identified due to lack of spectral data; it is crucial that these fundamental molecular spectra are obtained, either through experimental measurements (e.g., Gordon et al. 2017) or theoretical calculations (e.g., Tennyson et al. 2016; Fortenberry et al. 2019; Sousa-Silva et al. 2019).

3. Properties of Exocomets

Detections of known or suspected exocomets cover a wide variety of systems and techniques. We summarize the current small body nomenclature and propose a definition for exocomets, by building on the phenomenological approach used for solar system comets. We then present the various lines of evidence for exocomets and highlight the most notable hosting systems.

3.1. Small Body Nomenclature

The properties of comets and other small bodies in the solar system are not strictly defined by the International Astronomical Union (IAU). Resolution 5A for its General Assembly XXVI in 2006 defined planets and dwarf planets. By exclusion, all other bodies, except satellites, orbiting the Sun were collectively defined as small solar system bodies. This population includes a broad variety of objects, including asteroids, Trojans, moons, Centaurs and comets. These classes are mostly defined by their dynamical properties such as their location in the solar system and their relation with Jupiter (Levison 1996). In practice, there is a strong phenomenological component to the qualification of small bodies. Objects are identified as comets when they show activity consisting of a cloud of gas and dust (coma) and/or tails of ions and/or dust. In that simple view, comets are active due to the sublimation of volatile ices while asteroids are rocky and do not show such activity. This phenomenological approach is not perfect; a small number of asteroids have been observed to demonstrate activity (i.e., mass loss) through a variety of non-volatile sublimation processes, including impacts, rotational spin up, and in some cases repeated comet-like activity driven by sublimation of refractory material (Jewitt et al. 2015). Comets can cease to show activity far away from the Sun or as an evolutionary end-state when volatiles near their surface are depleted (Jewitt 2004). Finally, different small body populations in the solar system may be connected as objects evolve dynamically and can thus technically change classification over time—for example objects that are now in the so called "scattered disk" may become Centaurs and eventually Jupiter Family Comets (Bernstein et al. 2004; Sarid et al. 2019).

The identification of an object as a comet, asteroid, Centaur, or even Kuiper Belt object depends on its location in the solar system architecture and these terms raise expectations about the nature of the small body considered. In this paper, we use the word "exocomet" to describe comets which orbit other stars than the Sun and which exhibit some form of observable activity such as the release of gas or dust, e.g., through a coma or tails of ions or dust. The term "FEBs" has been used extensively as a synonym for exocomets (e.g., Lagrange-Henri et al. 1992; Beust & Lissauer 1994), though this term is misleading: the activity in such objects is likely driven by sublimation rather than evaporation, and "falling" implies objects seen only prior to periastron, while objects are now also detected after periastron (e.g., Kiefer et al. 2014b) when they could be described as "rising." The variable gas absorption signatures described in Section 3.2.1 clearly indicate the presence of exocometary gas and are thus characterized as bonafide exocomets. The asymmetrical transit signatures observed photometrically thought to be caused by transiting dust tails (as described in Section 3.2.2). The presence of trace amounts of cold gas within debris disks surrounding nearby main-sequence stars is the product of the release of gas from exocometary ices (as described in Section 3.2.3). Observational evidence has opened up the possibility that exocomets may be accreting onto WDs (e.g., Xu et al. 2017) as observed indirectly through the analysis of WD atmospheres (see Section 3.2.4). This suggests the accreting bodies might in some cases show compositional properties akin to solar system comets which indicates the bodies might indeed represent their extra solar equivalents, although the accretion is more likely dominated by asteroids.

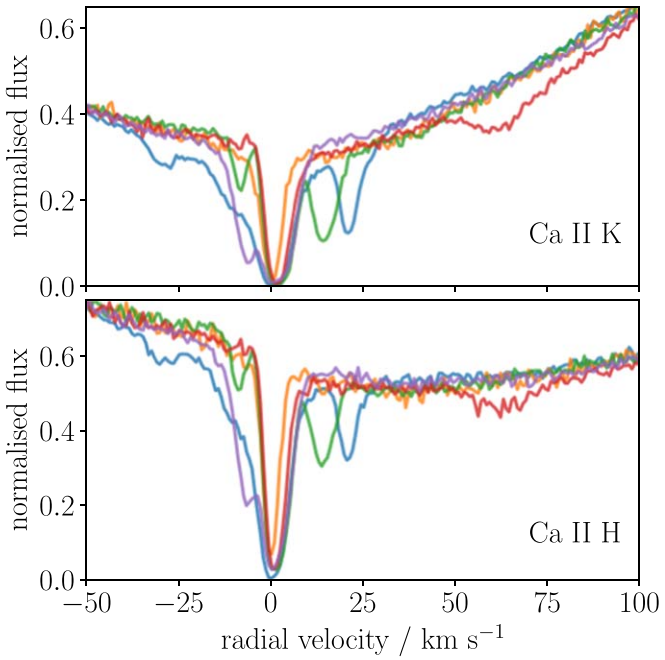

Figure 1. Ca II H & K line of the star β-Pic. The spectra (each shown in a different color) were obtained each at a different epoch using data from HARPS.
(A color version of this figure is available in the online journal.)

For cases where no cometary activity signatures are observed, we suggest the more inclusive term "Extrasolar Small Bodies" (ESBs). The properties of ESBs are not well constrained and we thus caution that what an object is identified as might later change as new information becomes available—a situation not uncommon for small bodies in our solar system.

3.2. Evidence for Exocomets

3.2.1. Spectroscopic Observations of Variable Absorption Lines

Exocomets can be discovered spectrocopically by the variable absorption they cause in addition to the stationary stellar Ca II H & K lines (see Figure 1). The absorption occurs when the exocometary gas passes in front of the star, absorbing part of the stellar light as it transits. The interstellar medium also causes absorption in addition to the exocomets. However, this absorption contribution remains constant when compared to the exocomet features which can vary from every few hours to a few times per month. Due to the small equivalent width (EW) of these variable exocomet features (few mÅ), only high-resolution instruments ($R > 60{,}000$; $\Delta v_r < 5\,\mathrm{km\,s^{-1}}$) are suitable for these observations.

β Pic is a young (~23 Myr) and bright ($V_{\mathrm{mag}} = 4$) A-star which exhibits the largest amount of exocometary activity of any star observed to date. Due to the edge-on inclination of the system as seen from Earth, β Pic is well positioned to detect exocomets in the same orbital plane, but much closer to the star than the debris disk observed at tens of au (e.g., Matrà et al. 2019b). The orbits of the exocomets around β Pic have been estimated indirectly using radial velocity observations combined with a physical sublimation model in an effort to calculate the stellocentric distance at transit (Beust et al. 1990; Beust & Tagger 1993). Rapidly varying absorption features (on the order of hours) are observed in sequential radial velocity spectra and are interpreted as being due to accelerating exocomets. The measured acceleration constrains the distance at which the exocomets pass in front of the star which is found to be within a few tens of stellar radii (Kennedy 2018). These observations are consistent with analytical estimates by Beust et al. (1996) who estimated that low-velocity Ca II absorption features correspond to distances of ~15–30 stellar radii (R_*) whereas high-velocity features correspond to distances of 5–8 R_*. At distances $\lesssim 3R_*$ the radiation pressure becomes too high for a large and thus detectable cloud to form. This is not the case for other lines such as Mg II and Al III where the radiation pressure is at least 10 times smaller (Beust et al. 1996). There is now a large set of β Pic spectra, routinely showing deep short term variations in several spectral lines including Ca II H & K in the visible and, for instance, Mg II and Fe II in the UV. There is a wide variety in the variable features' EW and velocities. They spread between -200 and $+200\,\mathrm{km\,s^{-1}}$ in radial velocity (see e.g., Kiefer et al. 2014b), and are in most cases redshifted compared to the star's Doppler shift, i.e., moving toward the central star. The redshift is due to the projection of the velocity of the exocomet onto the line of sight. These properties led the first discoverers of the β Pic phenomenon, to call them "FEBs," as discussed earlier. With the exception of the most conspicuous events in β Pic, they have EWs of a few mÅ. No system has been found yet (with the possible exception of ϕ Leo; Eiroa et al. 2016) with levels of variability comparable to the canonical case of β Pic. Their high frequency (hundreds of events per year) implies a large number of objects.

There are three exocomet hosting systems showing variable absorption features attributed to exocomets at both optical and UV wavelengths (see Table 1). The low number of objects is mainly due to the limited number of UV-facilities (recently only the Hubble Space Telescope (HST) is capable of UV-exocomet observations). Apart from β Pic, HD 172555 (Kiefer et al. 2014a; Grady et al. 2018) and 49 Cet (Miles et al. 2016), have shown exocometary-like absorption at both optical and UV wavelengths. Examples include the UV lines Fe II (e.g., Grady et al. 1996, 2018) and carbon or oxygen (Roberge et al. 2006, 2014; Grady et al. 2018) lines.

A few other systems have showed similar variable spectroscopic features (see e.g., Eiroa et al. 2016; Iglesias et al. 2018; Welsh & Montgomery 2018, and references therein) at optical wavelengths. The absorption features have predominantly been found when observing late B and A-type stars. The systems are

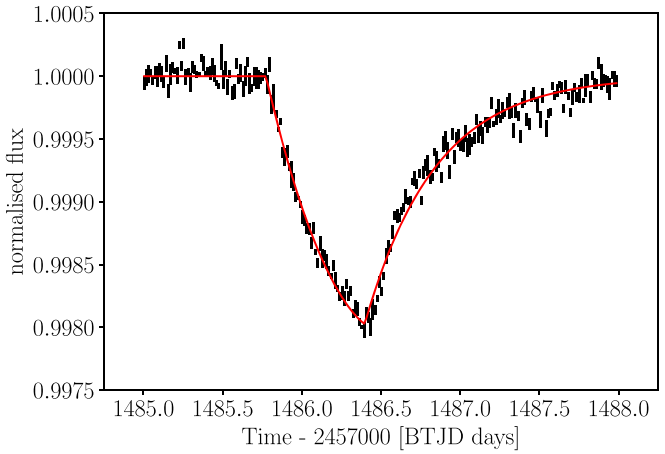

Figure 2. The typical transit shape of an exocomet when observed photometrically. The light curve has been binned to 20 minutes. The red line shows the best-fit model of an exponentially decaying optical depth tail convolved with the limb-darkened disk of the star. Figure adapted from Zieba et al. (2019).

(A color version of this figure is available in the online journal.)

all young with ages typically ranging from a few tens to hundred of million years old (see Wyatt et al. 2007b; Welsh & Montgomery 2018 and references therein). There is currently no clear explanation whether this is an observational bias or a physical effect. A possible exception, both in spectral type and age, is the 1.4 Gyr, F2V star η Crv where a tentative absorption signature (2.9σ detection) was detected by Welsh & Montgomery (2019). The majority of targets show possible exocomet induced variability in the Ca II H and/or K lines. With a limited number of observational epochs and lower signal to noise, their identification as exocometary, or at least circumstellar in origin is less certain than those of β Pic, 49 Cet and HD 172555. These candidate exocomet hosting systems which exhibit variability in one of the Ca II H or K lines or weak photometric signatures are listed in Table 2. All stars in this table require further follow-up to discard periodicity and ensure the variability is not caused by some other process (e.g., stellar pulsations).

3.2.2. Photometric Transit Observations

The milli-magnitude precision of space-based, wide field imagers such as Kepler/K2 and TESS have allowed the first detections of exocomets transiting other stars via photometry (Ansdell et al. 2018; Rappaport et al. 2018; Zieba et al. 2019). These transit events often have a distinct light curve shape reminiscent of a saw tooth whose shape depends on the angle of the trajectory. The shape was first predicted by Lecavelier Des Etangs et al. (1999), see Figure 2. The sharp decrease in flux is caused by a steep increase in absorption from the leading edge of the comet's coma followed by an exponential decay back to the full flux level of the star which is caused by the decreasing absorption from the cometary tail. This technique has proven the presence of comet-like bodies around stars with later spectral types (other than A-type), confirming the possible bias in the spectroscopic method. Estimating the size of exocomets is particularly hard due to the large number of degeneracies involved. As long as the exocometary orbital parameters remain unknown there is a large degeneracy between the transverse velocity, the length of the exocomet tail and the impact parameter (see Zieba et al. 2019).

3.2.3. Exocomet Populations within Debris Disks

The icy nuclei of exocomets presumably form in the outer regions of protoplanetary disks where conditions are cold enough to allow the freeze-out of volatile molecules and densities are still large enough for the growth of dust up to km-sized comets. These regions are also shielded from radiation from the young stellar object. At the end of planetary assembly, the icy exocomets may be left in one or more belts analogous to the asteroid and Kuiper belts in the solar system. In the extrasolar context, these reservoirs are known as debris disks, and are commonly observed through the dust and gas which is produced as their members collide and grind down (for a review, see Wyatt 2008; Hughes et al. 2018). Debris disks differ substantially from protoplanetary disks. Protoplanetary disks are much younger (typically <15 Myr old) and are orders of magnitude more massive in dust and gas, and solid objects are still growing due to the presence of large amounts of primordial gas dominating their dynamics (e.g., Wyatt et al. 2015). Debris disks on the other hand exist over a large range of ages and are typically dust-dominated. Observationally, debris disks are generally optically thin, whereas the more dust and gas rich protoplanetary disks are optically thick at visible wavelengths.

The large sensitivity advance and spatial resolution increase brought about by ALMA has recently allowed the detection of cold CO gas within belts around different stellar type stars (19 so far, e.g., Matrà et al. 2019a). Gas has also been detected in atomic form within debris disks, through far-IR/sub-mm emission lines of C I, C II and O I with Herschel and ALMA (e.g., Cataldi et al. 2014; Kral et al. 2016, 2019), but also through stable absorption lines seen against UV/optical stellar spectra at the stellar velocity (e.g., Lecavelier Des Etangs et al. 1997b, as opposed to red/blueshifted absorption due to star-grazing exocomets). These are only detectable for belts viewed edge-on (e.g., Rebollido et al. 2018), but allow comprehensive compositional inventories, as demonstrated by the large number of volatiles and metallic species detected in gas within the outer β Pic belt (e.g., Brandeker et al. 2004; Roberge et al. 2006).

Multiple component disks are often detected in debris disk systems. Most disks have dust temperatures colder than ~150–200 K (e.g., Chen et al. 2006; Lawler et al. 2009) although some stars (~20%, see the review by Kral et al. 2017a)

have a hot dust component (>300 K) within a few au, similar to the asteroid belt or zodiacal dust in the solar system (see Wyatt et al. 2007a and Absil et al. 2013). The F2V star η Corvi is a particularly interesting example as it is old (1.4 ± 0.3 Gyr, Nordström et al. 2004) and exhibits both a hot and cold dust component (e.g., Smith et al. 2009; Defrère et al. 2015). Using the Spitzer space telescope and the Infrared Telescope Facility/SPeX Lisse et al. (2012) observed η Corvi and found that the warm dust spectrum was consistent with very primitive cometary material. They concluded that the parent body or bodies would have been similar to Kuiper Belt Objects in the solar system which were likely prompted by dynamical stirring to spiral into the inner system. This idea is supported by ALMA observations where CO was detected and thought to originate from volatile rich solid material which sublimates and loses part of its volatiles as it crosses the H_2O or CO_2 snow lines (Marino et al. 2017).

While thermal desorption (i.e., sublimation) dominates gas release for solar system comets approaching the Sun, it is yet unclear which mechanism causes gas release within exocometary belts, since icy Kuiper Belt objects, for example, do not show significant evidence of outgassing (Jewitt et al. 2008; Stern & Trafton 2008; Stern et al. 2019). However, extrasolar belts with detected gas are typically much younger (10 to a few 100 Myr old), and at least 100 times more massive than the current Kuiper Belt. They are collision-dominated environments, where km-sized bodies produce a collisional cascade that extends down to micron-sized grains. Then, it is reasonable to assume that gas will also be released within this cascade, for example through resurfacing and the release of trapped volatile material, but also UV-stimulated photodesorption (e.g., Grigorieva et al. 2007; Öberg et al. 2009a, 2009b; Fillion et al. 2014; Martín-Doménech et al. 2015), or sublimation following high-velocity collisions of accelerated icy grains (Czechowski & Mann 2007).

Solar system comets can provide information on the dust properties of debris discs as dust in these disks is considered to be released from exocomets through collisions, i.e., of cometary origin (see Hughes et al. 2018, for a review). Scattered light observations, such as polarimetry, present an excellent opportunity to study the physical properties of the dust particles in orbit around stars as well as cometary dust in the solar system (Kolokolova et al. 2004). Polarimetric observations yield insights into the distribution of dust grain sizes as well as the spatial distribution from the degree and angle of polarization as function of wavelength, especially in the case of spatially resolved observations. Polarization maps of the AU Microscopii (AU Mic) debris disk suggest that the dust particles in the debris disk share a similarly porous structure to cometary dust in the solar system and that the grains' porosity may be primordial since the dust ring lies beyond the ice sublimation point (Graham et al. 2007). Analysis of observations of the dust distribution in the β Pic debris disk by Ahmic et al. (2009) showed that a two-disk model fit the data the best and also agree with previously reported disk asymmetries (Heap et al. 2000; Golimowski et al. 2006). They find that the two disks have dust replenishment times on the order of $\sim 10^4$ yr at a distance of $\sim$100 au which hint at the presence of planetesimals that are responsible for the production of second generation dust. Observations of dust produced through collisions can thus provide a viable way to study exocomets/debris discs whether it be observations of the IR emission (such as the observations of η Corvi) or scattered light (such as AU Mic and β Pic).

3.2.4. WD Pollution

Due to the strong gravitational field, heavy elements are not expected in the atmospheres of WDs (Jura & Young 2014). Elements heavier than He will sink out of the observable atmosphere on short timescales, much less than the cooling age of the WD (Koester 2009). Despite this, between 25% and 50% of single WDs are "polluted" by elements heavier than He, which implies the ongoing accretion of material (Zuckerman et al. 2003, 2010; Koester et al. 2014). It has been shown that planetary systems (planets and planetesimal belts) can survive the violent stages of stellar evolution to the WD phase (Bonsor et al. 2011; Debes et al. 2012; Veras 2016). The standard theory about what causes the "pollution" cites planetesimals being scattered inwards on to star grazing orbits. When these bodies cross the tidal disruption radius they disrupt and subsequently accrete onto the atmosphere of the WD (Debes & Sigurdsson 2002; Jura 2003; Farihi et al. 2010; Veras et al. 2014a).

The mass of the "polluting" bodies has been found to be similar to that of solar system asteroids (10^{16}–10^{23} kg) by analyzing the abundance of metals in the atmospheres of the WDs (Girven et al. 2012; Xu & Jura 2012; Veras 2016). However, the exact mass of the "polluting" bodies is difficult to determine as there may be material in a circumstellar reservoir that is yet to be accreted onto the WDs. Furthermore, the accreted material could originate from multiple bodies.

The presence of minor bodies in WD systems is not just implied from spectroscopic studies of the WD photosphere. Comet-like transits of material around WDs can cause large drops in the flux due to the WD's smaller size (compared to main sequence objects), making them easier to identify in the lightcurves. Two WDs have been observed with saw tooth transit features in their lightcurves. WD 1145+017 is a heavily polluted WD with numerous transits. The deepest transit of this WD has a period of roughly 4.5 hr and blocks 60% of the optical stellar flux (Vanderburg et al. 2015). This is likely from an actively disintegrating minor body in orbit. The WD ZTF J013906.17+524536.89 was found with transits separated by 110 days that caused a 30%–45% drop in the optical stellar flux (Vanderbosch et al. 2020). Also, one heavily polluted WD

(SDSS J122859.93+104033.0) shows evidence for an orbiting planetesimal within its circumstellar gas disk on a ∼2 hr orbit (Manser et al. 2019).

Spectroscopic observations of the atmospheres of "polluted" WDs can reveal the bulk compositions of the accreted planetary material. To date, 20 different heavy elements have been detected in polluted WDs: C, N, O, Na, Mg, Al, Si, P, S, Ca, Sc, Ti, V, Cr, Mn, Fe, Co, Ni, Cu and Sr (Zuckerman et al. 2007; Xu et al. 2013, 2017; Melis & Dufour 2017). There are more than 20 WDs with detailed abundance analyses and the composition of their pollutants are roughly akin to rocky objects in the solar system (e.g., Klein et al. 2010; Gänsicke et al. 2012; Harrison et al. 2018; Swan et al. 2019). So far, there is only one system (WD 1425+540) that has exhibited volatile-rich elements including N, C, and O with an elemental composition similar to the dust surrounding comet 1P/Halley (Xu et al. 2017).

A theoretical study by Veras et al. (2014b) found that the delivery of exo-Oort cloud comets onto WDs is dynamically possible, thus, it is not unexpected that WDs can be polluted by such objects. Further evidence for the accretion of comet-like material onto WDs comes from the atmospheres of He dominated WDs (also known as DB WDs). As comet-like material is rich in H, and H unlike all other elements never sinks out of atmosphere of a He dominated WD, the accretion of comet-like material produces a permanent signature in the atmosphere of such a WD. Atmospheric H in He dominated WDs therefore provides evidence for the historical accretion of comet-like bodies. Hollands et al. (2017, 2018) analyzed the chemical composition of 230 WDs with long cooling ages ($T_{\rm eff} < 9000$ K). They found that several of the objects showed large amounts of trace H, thus potentially accreted comet-like material in the past. WD 1425+540 along with the numerous He dominated WDs which contain a significant amount of trace H suggest that WDs may be polluted by analogues of solar system comets. In our own solar system the Sun is impacted by comets frequently with comets grazing the Sun every few days (Lamy et al. 2013) compared to asteroids which much less frequently graze the Sun (e.g., Gladman et al. 1997; Minton & Malhotra 2010). Therefore, it certainly seems possible that exocomets may impact other stars, including WDs. Further studies of polluted WDs may offer a unique insight into the bulk composition of exo-comets.

3.3. The Composition of Exocomets

Gas is released by exocomets transiting their host star at a few stellar radii as well as by the population of exocomets further out at tens of au within cold debris disks, giving us access to their composition. Several gas species attributed to the presence of exocomets have been detected to date (see Table A2).

At a few stellar radii, gas is thought to originate from sublimation as exocomets move away from or toward the star, producing red or blueshifted gas absorption lines. The most readily detected species is Ca^+, where absorption is seen in the H&K lines at 3933.7 Å and 3968.5 Å, respectively. The absorption signatures typically vary on timescales of hr to days relative to the absorption features caused by circumstellar and interstellar gas which vary on much longer timescales (Kiefer et al. 2019). Time-variable ultraviolet lines such as Al III, C II, C IV, Mg II, Fe I and Fe II have been detected in observations of β Pic (Deleuil et al. 1993; Vidal-Madjar et al. 1994; Miles et al. 2016; Grady et al. 2018), see Table A2 for a complete list of species. Although the star itself is unable to photoionize some of these species, it is thought that exocomets sufficiently close to the star (a few stellar radii) form a shock surface where the heat generated by compression and collisions is high enough to produce highly ionized atoms (Beust & Tagger 1993).

The connection between these red or blueshifted exocomets at a few stellar radii from their stars and the exocomets that are much more distant orbiting in exo-Kuiper belts (with lines at the stellar velocity, i.e., no shifts) is not clear. The most intuitive interpretation is that we are seeing the same sort of exocomets but at different locations, i.e., the shifted signatures of exocomets appear when the objects are pushed onto small pericentre orbits from large distances. There are dynamical processes that look promising at producing this inward flow of material (Beust & Morbidelli 1996, 2000; Bonsor et al. 2012, 2013, 2014; Faramaz et al. 2017; Marino et al. 2018; Sezestre et al. 2019). If this is correct, observations of gas released within debris disks at tens of au can be used to constrain the volatile content, while observations of transits close to the star probe the refractories within exocomets. Observations of exocometary gas within debris disks makes it possible to study the composition of the bulk exocomet population. Assuming the collisional cascade that is producing observable dust is also releasing gas at a steady-state, and that all the ice is lost to the gas phase by the time solids are ground down to the small grains (which are then ejected through radiation pressure), allows derivation of exocometary mass fractions of ice species within the debris disk (Zuckerman & Song 2012; Matrà et al. 2015; Kral et al. 2017b). In the systems where CO has been measured by ALMA, the CO (and/or CO_2) mass fraction in exocomets is consistent with solar system cometary compositions, within about an order of magnitude (Matrà et al. 2017). Searches for gas molecules other than CO are underway with ALMA, though these are harder to detect due to their significantly shorter photodissociation timescales (Matrà et al. 2018). Using the excitation of the observed O I line, Kral et al. (2016) quantified the maximum H_2O-to-CO ratio of exocomets within the β Pic debris disk and found that little water is released together with CO; this is consistent with

a direct upper limit on H_2O gas emission from Herschel (Cavallius et al. 2019).

Detectable CO release rates observed in debris disks vary by orders of magnitude from 10^{-1} to less than 10^{-4} $M_\oplus\,\mathrm{Myr}^{-1}$. Taking a typical production rate of 10^{-2} $M_\oplus\,\mathrm{Myr}^{-1}$, we find a production rate of $\sim 10^{34}$ CO molecules s^{-1}, which is much higher than what is observed in the solar system for a given comet (see Section 2.1). This is however not surprising, as the rate in debris disks arises from the collective release from a large amount of exocomets (as first proposed by Lecavelier Des Etangs et al. 1996 for the β Pic debris disk), rather than the sublimation-driven release by a single object typically observed in the solar system.

4. Observational Similarities and Differences Between Solar System Comets and Exocomets

4.1. Spatially Resolving (Exo)Comets

A major difference between the observations of solar system comets and exocomets is that the former are studied individually, whereas the latter generally cannot be resolved. Persistent and robotic observing campaigns have accrued chemical abundances for hundreds of comets for fragment species (A'Hearn et al. 1995; Fink 2009; Cochran et al. 2012), and for dozens of comets for molecules that are thought to be released directly from the nucleus (A'Hearn et al. 2012; Dello Russo et al. 2016). These surveys indicate that comets have a broad range of properties that are likely related to their origin in the protoplanetary disk (Davidsson et al. 2016; Eistrup et al. 2019), but that are also altered by solar heating and interstellar processing. The extent of these effects on comets, and the exact connection between volatiles stored in the nucleus and the observable coma are among the major questions in comet research (A'Hearn 2017; Keller & Kührt 2020). Similar to the comets of the solar system, exocomet likely also vary in chemical composition depending on their formation environments which is governed by their location in the debris disk and type of star in which they orbit.

For exocomets the determination of the properties of individual objects is a challenge as we can never be sure we are only observing a single object or collection of fragments originating from a single object. Some photometric and spectroscopic transits of exocomets indeed suggest the multiplicity of transiting objects (Beust et al. 1996; Kiefer et al. 2017; Neslušan & Budaj 2017). The exception to this are interstellar visitors (see Section 5) which can be studied individually. Photometric observations which show transit light curves consistent with what is expected from a single exocomet transit may increase the likelihood that a single exocomet is being characterized, although there is currently no method in place for verifying the single nature of photometrically detected exocomets. Observations of the gas in planetesimal belts likely measure the combined composition of large numbers of exocomets. Similarly, the elemental composition derived from WD pollution and spectroscopic observations is likely the product of multiple exocomets and therefore reflects the chemical properties of an entire population of objects.

4.2. Detection Methods

Exocomets can be detected through the gas and dust they release, producing absorption of starlight and/or emission. First, exocomets at a few stellar radii can be detected with high resolution spectrographs through their gas coma, which covers a significant fraction of the stellar surface and hence makes them detectable in absorption against the star (Lagrange-Henri et al. 1992). High resolving power is needed, as delivered by the current generation of optical and NIR echelle spectrographs have spectral resolutions of 120,000 (Mayor et al. 2003) to 190,000 (Pepe 2017). This allows measurement of the amount of absorption as a function of radial velocity at resolutions of $\sim$2–5 km s^{-1}. This is more than suitable for detecting exocomets which typically display red and blueshifted absorption signatures with a radial velocity in the range from 0 to $\pm$200 km s^{-1}.

Second, with the introduction of sensitive space based photometers such as Kepler/K2 and TESS, exocomets close to the star can also be detected by the light blocked out as the dust released from their surface transits the host star. Similar to exoplanets, which display a unique light curve as they transit, transiting exocomets produce their own unique light curve as shown in Section 3.2.2. This provides information about the dust density in the tail. They could also be potentially a source of false positives for single transiting exoplanets when their trajectory causes a symmetric lightcurve (see Lecavelier Des Etangs et al. 1999).

Third, exocomets further away from their host stars, orbiting within debris belts, can also be observed through the gas they release as part of the collisional cascade. This gas can be seen in absorption in the UV/optical for edge-on systems (e.g., Brandeker et al. 2004; Roberge et al. 2006) and in emission in the far-IR (e.g., CII, OI) or in the sub-mm (e.g., CO, C I).

Solar system comet nuclei are obscured when active, but their nuclei can be directly imaged (optical/IR/radar) when they are far from the Sun, weakly active, and/or very close to Earth. Similar observations of exocomet nuclei will not be possible for the foreseeable future. Even detections of transits by solid bodies will only be possible for bodies much larger than any minor bodies in the solar system. Currently, the detection of exocomet transits requires much higher optical depth than is seen for typical comets in the solar system. This suggests either large exocomets ($\sim$10–100 km), larger than most solar system comets (Bauer et al. 2017) but comparable to many Kuiper Belt objects (Schlichting et al. 2013) with extended dust tails transiting the star and/or a system containing a group of exocomets, possibly disintegrating.

Comet comae in the solar system are seen in emission. The only solar system comet successfully observed while transiting the Sun's disk was the sungrazer C/2011 N3. This was only observed for a few minutes in both absorption and emission at EUV wavelengths, before the comet was apparently destroyed (Schrijver et al. 2012). To date, direct spectroscopic exocomet detections have been entirely in absorption. Lines that are commonly bright in solar system comets (Na I in sungrazers and a few other comets further from the Sun with very high production rates, CN in regular comets; see Table A1) have been searched for in emission in exocomets without success. Spectroscopic observations of exocomets have not yet shown the presence of CN. The exception to this is 2I/Borisov which clearly showed CN emission (e.g., Fitzsimmons et al. 2019) while passing through our solar system. An overview of the cometary environments and how they are observed is presented in Figure 3.

4.3. Compositional Similarities and Differences

The Ca II lines commonly seen in the spectra of β Pic and polluted WDs (see Section 3.2) have been detected in the extreme case of the large sungrazing comet C/1965 S1 Ikeya–Seki (Preston 1967; Slaughter 1969). Interestingly, the typical optical cometary emission lines (CN, C_2, C_3, etc.) were faint or undetectable in Ikeya–Seki close to its perihelion; this behavior may provide insight into what is seen (or not seen) in exocomets close to their stars. Nitrogen-bearing molecules such as N_2, NH_3 and CN, although detectable in solar system comets, are considered minor constituents (e.g., Krankowsky et al. 1986; Eberhardt et al. 1987; Wyckoff et al. 1991). Observations of the NI line in β Pic showed no short term variable absorption signatures of NI which is consistent with N only being a minor exocometary consituent (Wilson et al. 2019).

The main volatile of most solar system comets is water ice. Observations of the Lyα emission line in β Pic showed a strong asymmetric line profile caused by additional redshifted absorption. The asymmetric line shape has been interpreted as hydrogen gas falling toward the star which may have arisen from the dissociation of water originating from sublimating exocomets (Wilson et al. 2017) or from the gas disk accreting onto the star (Kral et al. 2017b).

The Na D lines at 589.0 and 589.6 nm have been detected in over a dozen comets (Cremonese et al. 2002), primarily at heliocentric distances less than 1 au due to their very large fluorescence efficiencies for heliocentric velocities exceeding a few 10 s of km s^{-1} (Watanabe et al. 2003). Perhaps counter-intuitively, sodium has not conclusively been detected in close-in transiting exocomets. Observations of the Na D lines are challenging from the ground due to telluric contamination. Future observations to look for variable Na D lines in exocomets clearly warrants further investigation.

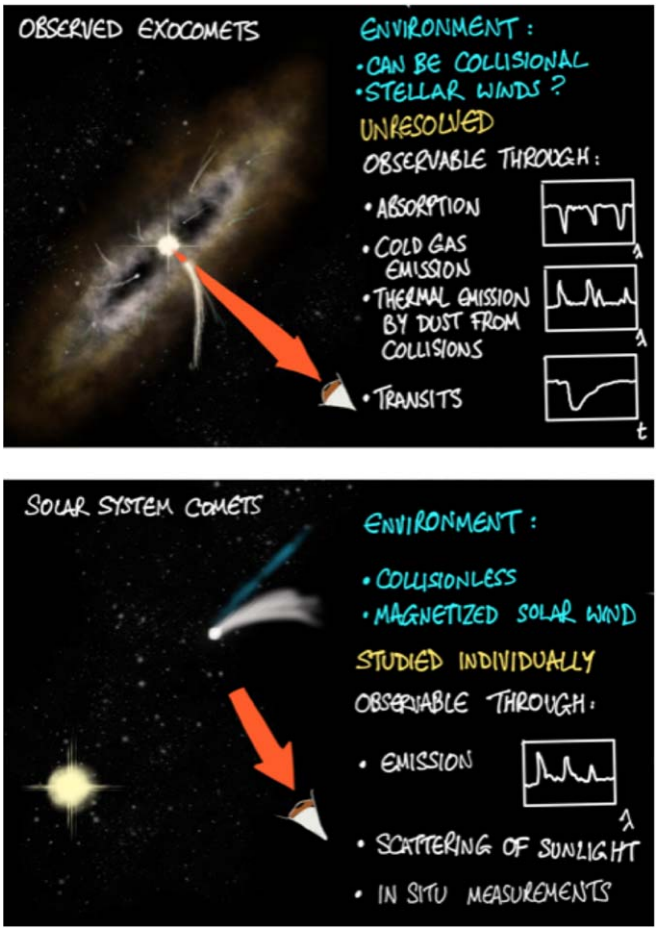

Figure 3. An overview of the environments and observational signatures of observed exocomets and solar system comets. The differences between the collisional gas environment in which observed exocomets generally reside and the collisionless interplanetary medium in our planetary system are covered in Section 4.3. The solar wind is a very well-characterized medium, whereas outflowing stellar winds in observed exocomets' systems, if they exist, are very poorly characterized. The latter are extremely difficult to detect, and it is unknown whether they carry a magnetic field.
(A color version of this figure is available in the online journal.)

No subsequent sungrazing comets have approached Ikeya–Seki's size or brightness, so we have yet to study such a comet with modern instrumentation for a more direct comparison to exocomets. Comet C/2012 S1 (ISON) held great promise for such observations, as it was discovered a year before perihelion and was the subject of a worldwide observing campaign. However, it evidently began disintegrating before perihelion (Knight & Battams 2014), and was undetected in the EUV around its perihelion passage (Bryans & Pesnell 2016). More than 4000 sungrazing comets have been detected to date (Battams & Knight 2017), but the vast majority are smaller than 100 m in diameter and only observed via broadband imaging (e.g., Knight et al. 2010). Limited spectroscopy of a dozen or so sungrazing comets has been obtained at UV and EUV wavelengths by solar

observatories over the last two decades (e.g., Bemporad et al. 2007; Bryans & Pesnell 2012; Schrijver et al. 2012). These observations were optimized for solar observing so the specific comet lines detected were serendipitous and not necessarily the most prominent or diagnostic. The detections of highly ionized O, C, and Fe by Solar Dynamics Observatory's AIA instrument (McCauley et al. 2013; Pesnell & Bryans 2014) hold promise for direct comparisons to exocomet systems since conditions are akin to star-grazing exocomet systems, but will likely require a future generation of space-based X-ray or UV facilities to be detected. The most highly ionized species attributed to exocomets are Al III, C IV and Si IV. Even higher ionized species may exist, but have not yet been detected. A model of cometary debris in the solar corona by Pesnell & Bryans (2014) opens up the possibility of detecting higher ionized species in exocomets (they model the detection of C IV, Fe VIII through Fe X, and O III through O VI. A review of observations of Near-Sun Comets in our solar system has been provided by Jones et al. (2018).

Solar system comet observations indicate that some intermediate charge state ions are created through photoionization, e.g., C III detected in C/2002 X5 (Kudo-Fujikawa) when it was at ∼0.2 au from the Sun can be explained by the double photoionization of C originating from cometary dust (Povich et al. 2003). To explain the presence of highly ionized species such as Al III and C IV in exocomet spectra, Beust & Tagger (1993) invoked the process of ionization at a collisional shock occurring around exocomets. This is because the central star (in this case β Pic) is unable to photoionize such highly ionized species. The heat generated by compression and collisions within the shock surface of exocomets sufficiently close to the star were thought to be high enough to explain the formation of the highly ionized ions.

Shocks have been detected in situ at numerous solar system comets during comet encounter missions (e.g., Gringauz et al. 1986; Neubauer et al. 1993; Coates et al. 1997; Gunell et al. 2018). These arise due to the slow-down and deflection of the supersonic solar wind when it reaches the cometary obstacle, where significant mass, in the form of freshly ionized cometary gas, is added to the wind. It is important to note that all solar wind shocks detected to date are collisionless rather than collisional; this is possible due to the presence of the heliospheric magnetic field that is carried by the solar wind.

Emission from higher ionization state species (Hydrogen and Helium-like ions) has been observed in solar system comets, too (Bodewits et al. 2007). Rather than being neutral species originating at the comet that are subsequently ionized, these ions' parent species originate at the Sun as multiply ionized heavy ions, e.g., $O^{7,8+}$, and are carried to the comet by the solar wind (Cravens 1997). Instead of moving to higher ionization states, these are partially neutralized at the comet through charge exchange processes with neutral species in the cometary coma, as described in Section 2.3. O IV was detected in situ in the ion tail of C/2006 P1 McNaught by the Ulysses spacecraft, but it is unclear whether that ion resulted from the ionization of cometary oxygen atoms, or the multistage neutralization of highly charged oxygen ions in the solar wind (Neugebauer et al. 2007).

Exocomets around stars with stellar winds could exhibit similar charge exchange emission at EUV and X-ray energies. This would be most apparent in charge states not expected in cold cometary environments. It is clear that stellar winds could be present at several of the systems where exocomets' presence has been inferred. Stellar winds are, however, difficult to detect; as noted by Suess & Tsurutani (2015), the Sun's solar wind would be invisible at stellar distances. The presence and nature of stellar winds in many of these systems will possibly remain undetermined. The conceivable presence of a stellar wind carrying a magnetic field, as is the case in our solar system, should be considered when interpreting observations of the ionized components of exocomets. A decoupling in the line-of-sight velocities of neutral and ionized components of an exocomet could indicate that the ions are carried by a magnetized stellar wind, i.e., as an ion tail.

Finally, as discussed in Sections 3.2.3 and 3.3, far-IR and millimeter observations of molecular emission lines within debris disks can be used to probe the composition of the population of exocomets within debris disks. The derived fractions of CO(+CO_2) ice by mass are so far found to be largely consistent with the compositions observed in solar system comets (Matrà et al. 2017), which may indicate similar formation conditions in the starting protoplanetary disks (A'Hearn et al. 2012; Eistrup et al. 2019). In addition to the CO(+CO_2) ice mass fractions, mm observations have started setting upper limits on CN emission, which (assuming CN is produced by HCN photodissociation alone) set tight constraints on the HCN/(CO+CO_2) outgassing rate ratio. This ratio is at the low end of what is expected from typical solar system HCN/(CO+CO_2) compositions in a few systems (Matrà et al. 2018; Kral et al. 2020). As mentioned in Section 3.3, upper limits on the presence of exocometary water vapor have also been set, directly (Cavallius et al. 2019) and indirectly (Kral et al. 2016), within the β Pic disk. These measurements suggest that the H_2O outgassing rate, when compared to that of CO(+CO_2), is, like HCN, also at the low end of solar system comet range. If depletions of water and HCN are widely confirmed compared to CO(+CO_2), this could imply either a true depletion of H_2O and HCN compared to CO(+CO_2) ice or, given the low temperatures of tens of K at these distances, decreased outgassing for the less volatile molecules of H_2O and HCN compared to CO (Matrà et al. 2018).

5. Interstellar Visitors

Dynamical models suggest that a large number of our comets (as much as 90%) was lost in the early solar system (Levison et al. 2010), and comets are still lost through continued

gravitational ejection. Similarly, other systems might eject their comets and these objects make it possible to study exocomets up close. Recently, two such interstellar objects were discovered when they passed through the solar system, 1I/'Oumuamua and 2I/Borisov (e.g., Fitzsimmons et al. 2019; 'Oumuamua ISSI Team 2019). The discovery of two such objects suggests that future discoveries will be relatively common (e.g., Trilling et al. 2017).

1I/'Oumuamua passed close to the Sun (0.25 au) and Earth (0.16 au), and its hyperbolic orbit confirmed its interstellar origins (Meech et al. 2017). Based on its brightness, the object's effective radius was likely less than 100 m, and the large amplitude of its lightcurve implies an extreme elongated or flattened shape (reviewed in 'Oumuamua ISSI Team 2019). Continued observations by HST indicated that its orbit was altered by non-gravitational forces, a clear indicator for sublimation-driven activity in comets (Micheli et al. 2018). However, no evidence of a coma or tail was observed and it has been argued that the typical drivers of activity in our solar system (H_2O, CO, or CO_2) could not have provided the observed non-gravitational acceleration for the assumed size and density (Sekanina 2019; Seligman & Laughlin 2020). As a result of these unusual properties, a number of models have been suggested that are well beyond the usual paradigm for the origin of comets and asteroids in our solar system. Several authors have suggested a combination of disruption and subsequent ejection from the host system of a large planetesimal during one or more close approaches to a giant planet, its host star, or one member of a low-mass binary (e.g., Ćuk 2018; Raymond et al. 2018b; Zhang & Lin 2020). Others report entirely new phenomena including an icy fractal aggregate (Moro-Martín 2019) or molecular hydrogen ice (Seligman & Laughlin 2020). Should future interstellar objects exhibit similar properties to 'Oumuamua, it may become necessary to rethink how typical our own solar system is.

When the second interstellar object, 2I/Borisov, was first discovered it already displayed a prominent tail, and subsequent archival searches in pre-discovery survey observations showed that it was active outside 5 au from the Sun (Ye et al. 2020). Borisov was brighter and observable for a much longer time than 'Oumuamua, and the emission of several fragment species common in solar system comets was observed, including CN, OH, C_2, [O I], and NH_2 (e.g., Fitzsimmons et al. 2019; Bannister et al. 2020; Lin et al. 2020; McKay et al. 2020; Xing et al. 2020). This initially led to the conclusion that many of the properties of this object were surprisingly similar to those of comets from our solar system. However, contemporaneous observations by HST, the Neil–Gehrels–Swift observatory, and ALMA allowed for the measurement of the production rates of two major parent volatiles, H_2O and CO (Bodewits et al. 2020; Cordiner et al. 2020). They found that the object contained substantially more CO ice than H_2O ice, with an abundance of at least 150%. This is very different from the CO to H_2O gas ratio observed in most comets in the inner solar system, which ranges between 0.2% and 23% and is typically around 4% (Bockelée-Morvan & Biver 2017). This high CO to H_2O ratio might be attributed to an origin in an environment significantly different from those in the early solar system, such as around an M-dwarf star (the most abundant type of star in our galaxy, but much cooler than the Sun, see Bodewits et al. 2020), or from the outer regions of a protoplanetary disk, far from its host star (Cordiner et al. 2020).

The European Space Agency has selected for launch in the late 2020s the *Comet Interceptor* mission (Snodgrass & Jones 2019) that could send multiple probes to an interstellar comet if a suitable target is discovered.[30] Although it is uncertain from where interstellar comets originate, they are likely to provide further insights into the similarities and differences between exocomets and solar system comets.

6. Summary and Outlook

In this paper we provide an overview of the observational properties of solar system comets and exocomets and compare their similarities and differences. Compared to solar system comets, the information we have about exocomets is very limited. While observations of exocomets are spatially unresolved and thus provide us with a holistic view, observations of solar system comets allow us to conduct in situ observations of individual cometary components (coma, dust tail, gas tail, nucleus) at high fidelity. Despite these challenges observations of exocometary gas around main sequence stars, "polluted" WD atmospheres as well as spectroscopic observations of transiting exocomets suggest that exocomets may not be that compositionally different to solar system comets. We assume that star and planet formation is a rather universal process, so a difference would not be that easy to explain, unless for example star/disk mass-ratios clearly differ for different targets. The detection of variable Ca II absorption lines and higher ionization state species—in exocomets, and solar system comets, along with the compositions found in some WD atmospheres—suggests that exocomets and comets share a similar composition. Solar system comets emit in high energy EUV and X-ray emission through the gradual neutralization of highly charged solar wind ions. Such processes may also occur at exocomets encountering stellar winds. The presence of shocks is also detected around exocomets through observations of the variable absorption lines of highly ionized species.

Observations of interstellar visitors such as 1I/'Oumuamua and 2I/Borisov allow us to learn about the physical and chemical properties of protoplanetary disks of distant stars, although their true systems of origin are unknown to us. Compositional studies of these objects might help link the

[30] http://www.cometinterceptor.space

fields of exocomets and solar system comets, and new studies of interstellar visitors hold the potential to further improve our understanding of the formation history of (exo)comets. Future observations of Na D lines in spectra of exocomet host stars will allow the similarities between exocomets and solar system comets to be tested. If the comets are indeed similar, we expect to see variable absorption signatures in the Na D lines. Multi-wavelength photometric monitoring observations of exocometary transits will provide more information about the dust properties such as the dust reflection as a function of wavelength. Space based photometric observations with TESS and Planetary Transits and Oscillations are likely to provide information about the extent of the exocometary tail and will yield rough estimates of the size of the exocomets. The James Webb Space Telescope opens up the possibility to look for new exocomet lines such as H_2O (6 μm), CH_4 (7.7 μm), C_2H_2 (13.7 μm), CO_2 (15 μm), and S I (25.2 μm) to mention a few. Present and upcoming research facilities, both for studies in and beyond our solar system, are expected to further bridge the cometary and exocometary science communities.

We thank the Lorentz Centre for facilitating the workshop "ExoComets: Understanding the Composition of Planetary Building Blocks" during 2019 May 13–17. The authors are grateful to the staff of the Lorentz Center for their assistance in arranging and running of the workshop, which led to the creation of this work. The authors would also like to thank Alain Lecavelier des Etangs, Grant Kennedy and Christopher Manser for feedback on the paper and for the fruitful discussions on the topic of exocomets and WDs. M.K. was supported by the University of Tartu ASTRA project 2014–2020.4.01.16-0029 KOMEET, financed by the EU European Regional Development Fund. F.K. acknowledge funding by PSL University Fellowship, and the Centre National d'Etudes Spatiales. G.H.J. is grateful to the UK Science and Technology Facilities Council for support through consolidated grant ST/S000240/1. D.I. acknowledges support from ICM (Iniciativa Científica Milenio) via Núcleo Milenio de Formación Planetaria. H.L. acknowledges support of the Netherlands Organisation for Scientific Reseach through the Planetary and Exo-Planetary Science (PEPSci) network. L.R. would like to acknowledge funding from The Science and Technology Facilities Council, Jesus College (Cambridge), and The University of Cambridge. Finally we would like to thank the anonymous referee for their very thorough review of this paper.

Appendix
Typical (Exo)cometary Spectroscopic Features

Table A1 below contains some of the most common cometary emission and absorption features seen in solar system comets. Table A2 contains a complete list of species showing variations which are attributed to the presence of exocomets.

Table A1
Typical Cometary Emission and Absorption Features Throughout the Electromagnetic Spectrum

Description	Wavelength	Spectral lines	Process	References
Gamma ray			No known emission	
X-ray and EUV	100 nm < 1 keV	Atomic ions (He II, C V, C VI, O VII),	Solar wind charge exchange	Bodewits et al. (2007)
		atomic ions (C II, C III)	Photoionization of atomic C	Povich et al. (2003)
Far UV	120–200 nm	Atoms (H, C, O),	Fluorescence, dissociative excitation,	Feldman et al. (2018)
		molecules CO, H_2	electron impact excitation	Weaver et al. (1981), Combi et al. (2011)
Mid and Near UV	200–380 nm	Molecules (CO), fragments (OH, CN),	Fluorescence, dissociative excitation,	Weaver et al. (1981), Feldman et al. (2004)
		molecular ions (CO^+, CO_2^+)	electron impact excitation	
Visible	380–700 nm	Fragment species (fragments C_2, C_3, NH_2 and atoms, O)	Fluorescence, dissociative excitation,	Cochran & Cochran (2002)
		molecular ions (H_2O^+), reflected sunlight	electron impact excitation	Preston (1967), Slaughter (1969)
		Ca II and Na I (primarily for sungrazers)		Cremonese et al. (2002), Douglas (1951)
Near IR	700 nm–5 μm	Dust, ice,	Reflected sunlight, Fluorescence	Ootsubo et al. (2012)
		Parent molecules (CO_2, H_2O, CO, CH_3OH),	electron impact excitation,	Dello Russo et al. (2016)
		molecular ions (CO_2^+), radicals (OH)	ice/mineral solid state absorption	Protopapa et al. (2014)
Mid IR	5–25 μm	Nucleus and dust	Thermal emission	Fernández et al. (2013)
			mineral solid-state absorption	
Far IR	25–200 μm	H_2O, HDO, NH_3, water-ice	Radiative and collisional excitation	Lellouch et al. (1998)
			thermal emission	

Table A1
(Continued)

Description	Wavelength	Spectral lines	Process	References
Sub-millimeter	200 μm–1 mm	Molecules (e.g., HCN, HNC, CO, CH_3OH, HDO, complex organics), dust	Radiative and collisional excitation thermal emission	Cordiner et al. (2014) Hartogh et al. (2011) Biver & Bockelée-Morvan (2019) Bockelée-Morvan et al. (2004)
Microwave	1 mm–10 cm	Molecules, ions, radicals (e.g., HCN, HCO^+, C_2H, CS)	Radiative and collisional excitation	Milam et al. (2004)
Radio	>10 cm	Molecules and radicals (OH, NH_3, H_2CO)	Radiative and collisional excitation	Crovisier et al. (2002) Howell et al. (2007)

Table A2
Detected Exocometary Absorption and Emission Features

Description	Wavelength	Spectral Lines	Process	References
Far UV	120–200 nm	Al II, Al III, C I, C II, C II*, C III, C IV, Si I, Si III, Si IV, O I	Exocometary bow shock at a few stellar radii and sublimation of dust grains	Deleuil et al. (1993), Vidal-Madjar et al. (1994) Miles et al. (2016), Grady et al. (2018)
		Ni II, S I, N I, CO	Molecules and photodissociation products from release in exocometary belts	Lagrange et al. (1998), Wilson et al. (2019) Roberge et al. (2000)
Mid and Near UV	200–400 nm	Mg II, Fe I, Fe II, Cr II, Mn II, Zn II,	Sublimation of dust grains at several tens of stellar radii	Vidal-Madjar et al. (1994), Kiefer et al. (2019) Lagrange et al. (1998)
Visible	380–700 nm	Ca II, Na I,	Sublimation of dust grains at several tens of stellar radii. Gas release in exocometary belts (Na I)	Ferlet et al. (1987), Brandeker et al. (2004)
Far IR	25–200 μm	O I, C II	Photodissociation of CO in exocometary belts forming neutral oxygen and ionized carbon	Cataldi et al. (2014), Kral et al. (2016)
Sub-millimeter	500 μm–1.3 mm	CI, CO	Cold CO produced in collisionally active exocometary belts and its photodissociation product neutral carbon	Moór et al. (2017), Higuchi et al. (2017) Kral et al. (2019)

ORCID iDs

Paul A. Strøm https://orcid.org/0000-0002-7823-1090
Dennis Bodewits https://orcid.org/0000-0002-2668-7248
Matthew M. Knight https://orcid.org/0000-0003-2781-6897
Flavien Kiefer https://orcid.org/0000-0001-9129-4929
Geraint H. Jones https://orcid.org/0000-0002-5859-1136
Quentin Kral https://orcid.org/0000-0001-6527-4684
Luca Matrà https://orcid.org/0000-0003-4705-3188
Eva Bodman https://orcid.org/0000-0002-4133-5216
Maria Teresa Capria https://orcid.org/0000-0002-9814-9588
Ilsedore Cleeves https://orcid.org/0000-0003-2076-8001
Alan Fitzsimmons https://orcid.org/0000-0003-0250-9911
Nader Haghighipour https://orcid.org/0000-0002-5234-6375
John H. D. Harrison https://orcid.org/0000-0002-9971-4956
Daniela Iglesias https://orcid.org/0000-0002-0756-9836
Mihkel Kama https://orcid.org/0000-0003-0065-7267
Harold Linnartz https://orcid.org/0000-0002-8322-3538
Liton Majumdar https://orcid.org/0000-0001-7031-8039
Ernst J. W. de Mooij https://orcid.org/0000-0001-6391-9266
Stefanie N. Milam https://orcid.org/0000-0001-7694-4129
Cyrielle Opitom https://orcid.org/0000-0002-9298-7484
Isabel Rebollido https://orcid.org/0000-0002-4388-6417

Laura K. Rogers https://orcid.org/0000-0002-3553-9474
Colin Snodgrass https://orcid.org/0000-0001-9328-2905
Clara Sousa-Silva https://orcid.org/0000-0002-7853-6871
Siyi Xu (许偲艺) https://orcid.org/0000-0002-8808-4282
Zhong-Yi Lin https://orcid.org/0000-0003-3827-8991
Sebastian Zieba https://orcid.org/0000-0003-0562-6750

References

A'Hearn, M. F. 2017, RSPTA, 375, 20160261
A'Hearn, M. F., Belton, M. J. S., Delamere, W. A., et al. 2011, Sci, 332, 1396
A'Hearn, M. F., Feaga, L. M., Keller, H. U., et al. 2012, ApJ, 758, 29
A'Hearn, M. F., Millis, R. C., Schleicher, D. O., Osip, D. J., & Birch, P. V. 1995, Icar, 118, 223
Absil, O., Defrère, D., Coudé du Foresto, V., et al. 2013, A&A, 555, A104
Agarwal, J., Della Corte, V., Feldman, P. D., et al. 2017, MNRAS, 469, s606
Ahmic, M., Croll, B., & Artymowicz, P. 2009, ApJ, 705, 529
Alibert, Y., Venturini, J., Helled, R., et al. 2018, NatAs, 2, 873
Altwegg, K., Balsiger, H., Bar-Nun, A., et al. 2015, Sci, 347, 1261952
Altwegg, K., Balsiger, H., Bar-Nun, A., et al. 2016, SciA, 2, e1600285
Altwegg, K., Balsiger, H., & Fuselier, S. A. 2019, ARA&A, 57, 113
Altwegg, K. & ROSINA Team 2018, in IAU Symp., Astrochemistry VII: Through the Cosmos from Galaxies to Planets, Vol. 332, ed. M. Cunningham, T. Millar, & Y. Aikawa, 153
Ansdell, M., Ioannou, Y., Osborn, H. P., et al. 2018, ApJL, 869, L7
Balsiger, H., Altwegg, K., Bar-Nun, A., et al. 2015, SciA, 1, e1500377
Bannister, M. T., Opitom, C., Fitzsimmons, A., et al. 2020, arXiv:2001.11605
Bardyn, A., Baklouti, D., Cottin, H., et al. 2017, MNRAS, 469, S712
Battams, K., & Knight, M. M. 2017, RSPTA, 375, 20160257
Bauer, J. M., Grav, T., Fernández, Y. R., et al. 2017, AJ, 154, 53
Bemporad, A., Poletto, G., Raymond, J., & Giordano, S. 2007, P&SS, 55, 1021
Bernstein, G. M., Trilling, D. E., Allen, R. L., et al. 2004, AJ, 128, 1364
Bertini, I., La Forgia, F., Tubiana, C., et al. 2017, MNRAS, 469, S404
Beust, H., Lagrange, A. M., Plazy, F., & Mouillet, D. 1996, A&A, 310, 181
Beust, H., Lagrange-Henri, A. M., Madjar, A. V., & Ferlet, R. 1990, A&A, 236, 202
Beust, H., & Lissauer, J. J. 1994, A&A, 282, 804
Beust, H., & Morbidelli, A. 1996, Icar, 120, 358
Beust, H., & Morbidelli, A. 2000, Icar, 143, 170
Beust, H., & Tagger, M. 1993, Icar, 106, 42
Bieler, A., Altwegg, K., Balsiger, H., et al. 2015, Natur, 526, 678
Bitsch, B., Izidoro, A., Johansen, A., et al. 2019, A&A, 623, A88
Bitsch, B., Lambrechts, M., & Johansen, A. 2015, A&A, 582, A112
Biver, N., & Bockelée-Morvan, D. 2019, ESC, 3, 1550
Biver, N., Bockelée-Morvan, D., Colom, P., et al. 1997, EM&P, 78, 5
Biver, N., Bockelée-Morvan, D., Moreno, R., et al. 2015, SciA, 1, 1500863
Bockelée-Morvan, D., & Biver, N. 2017, RSPTA, 375, 20160252
Bockelée-Morvan, D., Crovisier, J., Mumma, M. J., & Weaver, H. A. 2004, in The Composition of Cometary Volatiles, ed. M. C. Festou, H. U. Keller, & H. A. Weaver (Tuscon, AZ: Univ. Arizona Press), 391
Bodewits, D., Christian, D. J., Torney, M., et al. 2007, A&A, 469, 1183
Bodewits, D., Farnham, T. L., A'Hearn, M. F., et al. 2014, ApJ, 786, 48
Bodewits, D., Lara, L. M., A'Hearn, M. F., et al. 2016, AJ, 152, 130
Bodewits, D., Noonan, J. W., Feldman, P. D., et al. 2020, NatAs, 0, 85
Bodman, E. H. L., & Quillen, A. 2016, ApJL, 819, L34
Bonev, B. P., Villanueva, G. L., Paganini, L., et al. 2013, Icar, 222, 740
Bonsor, A., Augereau, J. C., & Thébault, P. 2012, A&A, 548, A104
Bonsor, A., Mustill, A., & Wyatt, M. C. 2011, MNRAS, 414, 930
Bonsor, A., Raymond, S. N., & Augereau, J.-C. 2013, MNRAS, 433, 2938
Bonsor, A., Raymond, S. N., Augereau, J.-C., & Ormel, C. W. 2014, MNRAS, 441, 2380
Boyajian, T. S., LaCourse, D. M., Rappaport, S. A., et al. 2016, MNRAS, 457, 3988
Brandeker, A., Liseau, R., Olofsson, G., & Fridlund, M. 2004, A&A, 413, 681
Brown, M. E., Bouchez, A. H., Spinrad, A. H., & Johns-Krull, C. M. 1996, AJ, 112, 1197
Brownlee, D. 2014, AREPS, 42, 179
Bryans, P., & Pesnell, W. D. 2012, ApJ, 760, 18
Bryans, P., & Pesnell, W. D. 2016, ApJ, 822, 77
Burke, D. J., & Brown, W. A. 2010, PCCP, 12, 5947
Cataldi, G., Brandeker, A., Olofsson, G., et al. 2014, A&A, 563, A66
Cavallius, M., Cataldi, G., Brandeker, A., et al. 2019, A&A, 628, A127
Chen, C. H., Sargent, B. A., Bohac, C., et al. 2006, ApJS, 166, 351
Cheng, K.-P., & Neff, J. E. 2003, AJ, 125, 868
Choukroun, M., Altwegg, K., Kührt, E., et al. 2020, SSRv, 216, 44
Coates, A. J., Mazelle, C., & Neubauer, F. M. 1997, JGR, 102, 7105
Cochran, A. L., Barker, E. S., & Gray, C. L. 2012, Icar, 218, 144
Cochran, A. L., & Cochran, W. D. 1991, Icar, 90, 172
Cochran, A. L., & Cochran, W. D. 2002, Icar, 157, 297
Cochran, A. L., Levasseur-Regourd, A.-C., Cordiner, M., et al. 2015, SSRv, 197, 9
Combi, M., Shou, Y., Fougere, N., et al. 2020, Icar, 335, 113421
Combi, M. R., Lee, Y., Patel, T. S., et al. 2011, AJ, 141, 128
Cordiner, M. A., Boissier, J., Charnley, S. B., et al. 2017, ApJ, 838, 147
Cordiner, M. A., Milam, S. N., Biver, N., et al. 2020, NatAs, 0, 84
Cordiner, M. A., Remijan, A. J., Boissier, J., et al. 2014, ApJL, 792, L2
Cravens, T. E. 1991, in IAU Coll., Plasma Processes in the Inner Coma, Vol. 167, ed. J. Newburn, R. L. M. Neugebauer, & J. Rahe, 1211
Cravens, T. E. 1997, GeoRL, 24, 105
Cremonese, G. 1999, SSRv, 90, 83
Cremonese, G., Huebner, W. F., Rauer, H., & Boice, D. C. 2002, AdSpR, 29, 1187
Crovisier, J., Colom, P., Gérard, E., Bockelée-Morvan, D., & Bourgois, G. 2002, A&A, 393, 1053
Ćuk, M. 2018, ApJL, 852, L15
Czechowski, A., & Mann, I. 2007, ApJ, 660, 1541
Davidsson, B. J. R., Sierks, H., Güttler, C., et al. 2016, A&A, 592, A63
Debes, J. H., & Sigurdsson, S. 2002, ApJ, 572, 556
Debes, J. H., Walsh, K. J., & Stark, C. 2012, ApJ, 747, 148
Deeg, H. J., Alonso, R., Nespral, D., & Boyajian, T. S. 2018, A&A, 610, L12
Defrère, D., Hinz, P. M., Skemer, A. J., et al. 2015, ApJ, 799, 42
Deleuil, M., Gry, C., Lagrange-Henri, A. M., et al. 1993, A&A, 267, 187
Dello Russo, N., Kawakita, H., Vervack, R. J., & Weaver, H. A. 2016, Icar, 278, 301
Douglas, A. E. 1951, ApJ, 114, 466
Drahus, M., Küppers, M., Jarchow, C., et al. 2010, A&A, 510, A55
Eberhardt, P., Krankowsky, D., Schulte, W., et al. 1987, A&A, 187, 481
Eiroa, C., Rebollido, I., Montesinos, B., et al. 2016, A&A, 594, L1
Eistrup, C., Walsh, C., & van Dishoeck, E. F. 2019, A&A, 629, A84
Ellinger, Y., Pauzat, F., Mousis, O., et al. 2015, ApJL, 801, L30
Faramaz, V., Ertel, S., Booth, M., Cuadra, J., & Simmonds, C. 2017, MNRAS, 465, 2352
Farihi, J., Barstow, M., Redfield, S., Dufour, P., & Hambly, N. 2010, MNRAS, 404, 2123
Farnham, T. L., Schleicher, D. G., & A'Hearn, M. F. 2000, Icar, 147, 180
Feldman, P. D., A'Hearn, M. F., Bertaux, J.-L., et al. 2015, A&A, 583, A8
Feldman, P. D., Cochran, A. L., & Combi, M. R. 2004, in Spectroscopic Investigations of Fragment Species in the Coma, ed. M. C. Festou, H. U. Keller, & H. A. Weaver, 425
Feldman, p. D., Weaver, H. A., A'Hearn, M. F., Combi, M. R., & Dello Russo, N. 2018, AJ, 155, 193
Ferlet, R., Hobbs, L. M., & Madjar, A. V. 1987, A&A, 185, 267
Fernández, Y. R., Kelley, M. S., Lamy, P. L., et al. 2013, Icar, 226, 1138
Festou, M. C. 1981, A&A, 95, 69
Fillion, J.-H., Fayolle, E. C., Michaut, X., et al. 2014, FaDi, 168, 533
Fink, U. 2009, Icar, 201, 311
Finson, M. J., & Probstein, R. F. 1968, ApJ, 154, 327
Fitzsimmons, A., Hainaut, O., Meech, K., et al. 2019, ApJ, 885, L9
Fortenberry, R. C., Peters, D., Ferrari, B. C., & Bennett, C. J. 2019, ApJL, 886, L10
Fulle, M., Blum, J., Green, S. F., et al. 2019, MNRAS, 482, 3326
Fulle, M., Della Corte, V., Rotundi, A., et al. 2017, MNRAS, 469, S45
Gänsicke, B. T., Koester, D., Farihi, J., et al. 2012, MNRAS, 424, 333
Girven, J., Brinkworth, C., Farihi, J., et al. 2012, ApJ, 749, 154
Gladman, B. J., Migliorini, F., Morbidelli, A., et al. 1997, Sci, 277, 197
Golimowski, D. A., Ardila, D. R., Krist, J. E., et al. 2006, AJ, 131, 3109
Gordon, I. E., Rothman, L. S., Hill, C., et al. 2017, JQSRT, 203, 3

Grady, C. A., Brown, A., Welsh, B., et al. 2018, AJ, 155, 242
Grady, C. A., Perez, M. R., Talavera, A., et al. 1996, ApJL, 471, L49
Graham, J. R., Kalas, P. G., & Matthews, B. C. 2007, ApJ, 654, 595
Grigorieva, A., Thébault, P., Artymowicz, P., & Brandeker, A. 2007, A&A, 475, 755
Gringauz, K. I., Gombosi, T. I., Remizov, A. P., et al. 1986, Natur, 321, 282
Guilbert-Lepoutre, A. 2012, AJ, 144, 97
Gunell, H., Goetz, C., Simon Wedlund, C., et al. 2018, A&A, 619, L2
Guzik, P., Drahus, M., Rusek, K., et al. 2019, NatAs, 4, 53
Harrison, J. H., Bonsor, A., & Madhusudhan, N. 2018, MNRAS, 479, 3814
Hartogh, P., Lis, D. C., Bockelée-Morvan, D., et al. 2011, Natur, 478, 218
Heap, S. R., Lindler, D. J., Lanz, T. M., et al. 2000, ApJ, 539, 435
Hempel, M., & Schmitt, J. H. M. M. 2003, A&A, 408, 971
Higuchi, A. E., Sato, A., Tsukagoshi, T., et al. 2017, ApJL, 839, L14
Hollands, M. A., Gänsicke, B. T., & Koester, D. 2018, MNRAS, 477, 93
Hollands, M. A., Koester, D., Alekseev, V., Herbert, E. L., & Gänsicke, B. T. 2017, MNRAS, 467, 4970
Howell, E. S., Lovell, A. J., Butler, B., & Schloerb, F. P. 2007, Icar, 191, 469
Huggins, W. 1881, RSPS, 33, 1
Hughes, A. M., Duchêne, G., & Matthews, B. C. 2018, ARA&A, 56, 541
Hui, M. T. 2013, MNRAS, 436, 1564
Iglesias, D., Bayo, A., Olofsson, J., et al. 2018, MNRAS, 480, 488
Iglesias, D. P., Olofsson, J., Bayo, A., et al. 2019, MNRAS, 490, 5218
Jewitt, D., Agarwal, J., Hui, M.-T., et al. 2019, AJ, 157, 65
Jewitt, D., Garland, C. A., & Aussel, H. 2008, AJ, 135, 400
Jewitt, D., Hsieh, H., & Agarwal, J. 2015, Asteroids IV (Tucson, AZ: Univ. Arizona Press), 221
Jewitt, D., & Li, J. 2010, AJ, 140, 1519
Jewitt, D. C. 2004, in From Cradle to Grave: The Rise and Demise of the Comets, ed. M. C. Festou, H. U. Keller, & H. A. Weaver, 659
Jin, Z., & Bose, M. 2019, SciA, 5, eaav8106
Jones, G. H., Knight, M. M., Battams, K., et al. 2018, SSRv, 214, 20
Jura, M. 2003, ApJL, 584, L91
Jura, M. 2006, ApJ, 653, 613
Jura, M., & Young, E. 2014, AREPS, 42, 45
Keller, H. U., & Kührt, E. 2020, SSRv, 216, 14
Kennedy, G. M. 2018, MNRAS, 479, 1997
Kennedy, G. M., Hope, G., Hodgkin, S. T., & Wyatt, M. C. 2019, MNRAS, 482, 5587
Kiefer, F., Lecavelier des Etangs, A., Augereau, J. C., et al. 2014a, A&A, 561, L10
Kiefer, F., Lecavelier des Etangs, A., Boissier, J., et al. 2014b, Natur, 514, 462
Kiefer, F., Lecavelier des Étangs, A., Vidal-Madjar, A., et al. 2017, A&A, 608, A132
Kiefer, F., Vidal-Madjar, A., Lecavelier des Etangs, A., et al. 2019, A&A, 621, A58
Klein, B., Jura, M., Koester, D., Zuckerman, B., & Melis, C. 2010, ApJ, 709, 950
Knight, M. M., A'Hearn, M. F., Biesecker, D. A., et al. 2010, AJ, 139, 926
Knight, M. M., & Battams, K. 2014, ApJL, 782, L37
Koester, D. 2009, A&A, 498, 517
Koester, D., Gaensicke, B. T., & Farihi, J. 2014, A&A, 566, A34
Kolokolova, L., Hanner, M. S., Levasseur-Regourd, A. C., & Gustafson, B. Å. S. 2004, in Physical Properties of Cometary Dust from Light Scattering and Thermal Emission, ed. M. C. Festou, H. U. Keller, & H. A. Weaver (Tucson, AZ: Univ. Arizona Press), 577
Kral, Q., Davoult, J., & Charnay, B. 2020, NatAs, 0, 66
Kral, Q., Krivov, A. V., Defrère, D., et al. 2017a, AstRv, 13, 69
Kral, Q., Marino, S., Wyatt, M. C., Kama, M., & Matrà, L. 2019, MNRAS, 489, 3670
Kral, Q., Matrà, L., Wyatt, M. C., & Kennedy, G. M. 2017b, MNRAS, 469, 521
Kral, Q., Wyatt, M., Carswell, R. F., et al. 2016, MNRAS, 461, 845
Kramer, E. A., Fernandez, Y. R., Lisse, C. M., Kelley, M. S. P., & Woodney, L. M. 2014, Icar, 236, 136
Krankowsky, D., Lammerzahl, P., Herrwerth, I., et al. 1986, Natur, 321, 326
Krasnopolsky, V. A., Mumma, M. J., Abbott, M. J., et al. 1997, Sci, 277, 1488
Lagrange, A. M., Beust, H., Mouillet, D., et al. 1998, A&A, 330, 1091
Lagrange-Henri, A. M., Beust, H., Ferlet, R., Vidal-Madjar, A., & Hobbs, L. M. 1990a, A&A, 227, L13
Lagrange-Henri, A. M., Ferlet, R., Vidal-Madjar, A., et al. 1990b, A&AS, 85, 1089
Lagrange-Henri, A. M., Gosset, E., Beust, H., Ferlet, R., & Vidal-Madjar, A. 1992, A&A, 264, 637
Lambrechts, M., & Johansen, A. 2014, A&A, 572, A107
Lamy, P., Faury, G., Llebaria, A., et al. 2013, Icar, 226, 1350
Lawler, S. M., Beichman, C. A., Bryden, G., et al. 2009, ApJ, 705, 89
Leblanc, F., Fulle, M., López Ariste, A., et al. 2008, A&A, 482, 293
Lecavelier Des Etangs, A. 1999, A&AS, 140, 15
Lecavelier Des Etangs, A., Deleuil, M., Vidal-Madjar, A., et al. 1997a, A&A, 325, 228
Lecavelier Des Etangs, A., Vidal-Madjar, A., Backman, D. E., et al. 1997b, A&A, 321, L39
Lecavelier Des Etangs, A., Vidal-Madjar, A., & Ferlet, R. 1996, A&A, 307, 542
Lecavelier Des Etangs, A., Vidal-Madjar, A., & Ferlet, R. 1999, A&A, 343, 916
Lellouch, E., Crovisier, J., Lim, T., et al. 1998, A&A, 339, L9
Levison, H. F. 1996, in ASP Conf. Ser. 107, Completing the Inventory of the Solar System, ed. T. Rettig & J. M. Hahn (San Francisco, CA: ASP), 173
Levison, H. F., Duncan, M. J., Brasser, R., & Kaufmann, D. E. 2010, Sci, 329, 187
Lin, H. W., Lee, C.-H., Gerdes, D. W., et al. 2020, ApJL, 889, L30
Lis, D. C., Bockelée-Morvan, D., Güsten, R., et al. 2019, A&A, 625, L5
Lissauer, J. J. 1993, ARA&A, 31, 129
Lisse, C. M., Dennerl, K., Englhauser, J., et al. 1996, Sci, 274, 205
Lisse, C. M., Wyatt, M. C., Chen, C. H., et al. 2012, ApJ, 747, 93
Lupu, R. E., Feldman, P. D., Weaver, H. A., & Tozzi, G.-P. 2007, ApJ, 670, 1473
Manser, C. J., Gänsicke, B. T., Eggl, S., et al. 2019, Sci, 364, 66
Marcus, J. N. 2007, ICQ, 29, 39
Marino, S., Bonsor, A., Wyatt, M. C., & Kral, Q. 2018, MNRAS, 479, 1651
Marino, S., Matrà, L., Stark, C., et al. 2016, MNRAS, 460, 2933
Marino, S., Wyatt, M. C., Panić, O., et al. 2017, MNRAS, 465, 2595
Martín-Doménech, R., Manzano-Santamaría, J., Muñoz Caro, G. M., et al. 2015, A&A, 584, A14
Marty, B., Altwegg, K., Balsiger, H., et al. 2017, Sci, 356, 1069
Matrà, L., MacGregor, M. A., Kalas, P., et al. 2017, ApJ, 842, 9
Matrà, L., Öberg, K. I., Wilner, D. J., Olofsson, J., & Bayo, A. 2019a, AJ, 157, 117
Matrà, L., Panić, O., Wyatt, M. C., & Dent, W. R. F. 2015, MNRAS, 447, 3936
Matrà, L., Wilner, D. J., Öberg, K. I., et al. 2018, ApJ, 853, 147
Matrà, L., Wyatt, M. C., Wilner, D. J., et al. 2019b, AJ, 157, 135
Mayor, M., Pepe, F., Queloz, D., et al. 2003, Msngr, 114, 20
McCauley, P. I., Saar, S. H., Raymond, J. C., Ko, Y.-K., & Saint-Hilaire, P. 2013, ApJ, 768, 161
McKay, A. J., Chanover, N. J., Morgenthaler, J. P., et al. 2013, Icar, 222, 684
McKay, A. J., Cochran, A. L., Dello Russo, N., & DiSanti, M. A. 2020, ApJL, 889, L10
Meech, K. J., & Svoren, J. 2004, in Using Cometary Activity to Trace the Physical and Chemical Evolution of Cometary Nuclei, ed. M. C. Festou, H. U. Keller, & H. A. Weaver (Tucson, AZ: Univ. Arizona Press), 317
Meech, K. J., Weryk, R., Micheli, M., et al. 2017, Natur, 552, 378
Melis, C., & Dufour, P. 2017, ApJ, 834, 1
Micheli, M., Farnocchia, D., Meech, K. J., et al. 2018, Natur, 559, 223
Milam, S. N., Savage, C., Ziurys, L. M., & Wyckoff, S. 2004, ApJ, 615, 1054
Miles, B. E., Roberge, A., & Welsh, B. 2016, ApJ, 824, 126
Minton, D. A., & Malhotra, R. 2010, Icar, 207, 744
Montesinos, B., Eiroa, C., Lillo-Box, J., et al. 2019, A&A, 629, A19
Montgomery, S. L., & Welsh, B. Y. 2012, PASP, 124, 1042
Montgomery, S. L., & Welsh, B. Y. 2017, MNRAS, 468, L55
Moór, A., Curé, M., Kóspál, Á, et al. 2017, ApJ, 849, 123
Moro-Martín, A. 2019, ApJL, 872, L32
Mullen, P. D., Cumbee, R. S., Lyons, D., et al. 2017, ApJ, 844, 7
Mumma, M. J., & Charnley, S. B. 2011, ARA&A, 49, 471
Neslušan, L., & Budaj, J. 2017, A&A, 600, A86
Neubauer, F. M., Marschall, H., Pohl, M., et al. 1993, A&A, 268, L5
Neugebauer, M., Gloeckler, G., Gosling, J. T., et al. 2007, ApJ, 667, 1262

Nordström, B., Mayor, M., Andersen, J., et al. 2004, A&A, 418, 989
Öberg, K. I., Linnartz, H., Visser, R., & van Dishoeck, E. F. 2009a, ApJ, 693, 1209
Öberg, K. I., van Dishoeck, E. F., & Linnartz, H. 2009b, A&A, 496, 281
Ootsubo, T., Kawakita, H., Hamada, S., et al. 2012, ApJ, 752, 15
Opitom, C., Fitzsimmons, A., Jehin, E., et al. 2019a, A&A, 631, L8
Opitom, C., Hutsemékers, D., Jehin, E., et al. 2019b, A&A, 624, A64
'Oumuamua ISSI Team, Bannister, M. T., Bhandare, A., et al. 2019, NatAs, 3, 594
Pepe, F. 2017, in ESO Calibration Workshop: The Second Generation VLT Instruments and Friends, 35, Zenodo, doi:10.5281/zenodo.887289
Pesnell, W. D., & Bryans, P. 2014, ApJ, 785, 50
Pollack, J. B., Hubickyj, O., Bodenheimer, P., et al. 1996, Icar, 124, 62
Povich, M. S., Raymond, J. C., Jones, G. H., et al. 2003, Sci, 302, 1949
Preston, G. W. 1967, ApJ, 147, 718
Prialnik, D., & Bar-Nun, A. 1987, ApJ, 313, 893
Price, O., Jones, G. H., Morrill, J., et al. 2019, Icar, 319, 540
Protopapa, S., sunshine, J. M., Feaga, L. M., et al. 2014, Icar, 238, 191
Rappaport, S., Vanderburg, A., Jacobs, T., et al. 2018, MNRAS, 474, 1453
Raymond, J. C., Downs, C., Knight, M. M., et al. 2018a, ApJ, 858, 19
Raymond, S. N., Armitage, P. J., & Veras, D. 2018b, ApJL, 856, L7
Rebollido, I., Eiroa, C., Montesinos, B., et al. 2018, A&A, 614, A3
Redfield, S. 2007, ApJL, 656, L97
Redfield, S., Kessler-Silacci, J. E., & Cieza, L. A. 2007, ApJ, 661, 944
Roberge, A., Feldman, P. D., Lagrange, A. M., et al. 2000, ApJ, 538, 904
Roberge, A., Feldman, P. D., Weinberger, A. J., Deleuil, M., & Bouret, J.-C. 2006, Natur, 441, 724
Roberge, A., & Weinberger, A. J. 2008, ApJ, 676, 509
Roberge, A., Welsh, B. Y., Kamp, I., Weinberger, A. J., & Grady, C. A. 2014, ApJL, 796, L11
Roth, L., Saur, J., Retherford, K. D., et al. 2014, Sci, 343, 171
Sarid, G., Volk, K., Steckloff, J. K., et al. 2019, ApJL, 883, L25
Schleicher, D. G., & Farnham, T. L. 2004, in Photometry and Imaging of the Coma with Narrowband Filters, ed. M. C. Festou, H. U. Keller, & H. A. Weaver (Tucson, AZ: Univ. Arizona Press), 449
Schleicher, D. G., Lederer, S. M., Millis, R. L., & Farnham, T. L. 1997, Sci, 275, 1913
Schlichting, H. E., Fuentes, C. I., & Trilling, D. E. 2013, AJ, 146, 36
Schrijver, C. J., Brown, J. C., Battams, K., et al. 2012, Sci, 335, 324
Schulz, R., Hilchenbach, M., Langevin, Y., et al. 2015, Natur, 518, 216
Sekanina, Z. 2019, arXiv:1905.00935
Seligman, D., & Laughlin, G. 2020, ApJ, 896, L8
Sezestre, É, Augereau, J. C., & Thébault, P. 2019, A&A, 626, A2
Slaughter, C. D. 1969, AJ, 74, 929
Smith, R., Wyatt, M. C., & Haniff, C. A. 2009, A&A, 503, 265
Snodgrass, C., & Jones, G. H. 2019, NatCo, 10, 5418
Sousa-Silva, C., Petkowski, J. J., & Seager, S. 2019, PCCP, 21, 18970
Stern, S. A., & Trafton, L. M. 2008, in The Solar System Beyond Neptune, ed. M. A. Barucci et al. (Tucson, AZ: Univ. Arizona Press), 365
Stern, S. A., Weaver, H. A., Spencer, J. R., et al. 2019, Sci, 364, eaaw9771
Suess, S., & Tsurutani, B. 2015, Encyclopedia of Atmospheric Sciences (Amsterdam: Elsevier), 189
Swan, A., Farihi, J., Koester, D., et al. 2019, MNRAS, 490, 202
Sykes, M. V., Grün, E., Reach, W. T., & Jenniskens, P. 2004, in The Interplanetary Dust Complex and Comets, ed. M. C. Festou, H. U. Keller, & H. A. Weaver (Tucson, AZ: Univ. Arizona Press), 677
Tennyson, J., Yurchenko, S. N., Al-Refaie, A. F., et al. 2016, JMoSp, 327, 73
Trilling, D. E., Robinson, T., Roegge, A., et al. 2017, ApJL, 850, L38
Vanderbosch, Z., Hermes, J., Dennihy, E., et al. 2020, ApJ, 897, 171
Vanderburg, A., Johnson, J. A., Rappaport, S., et al. 2015, Natur, 526, 546
Veras, D. 2016, RSOS, 3, 150571
Veras, D., Leinhardt, Z. M., Bonsor, A., & Gänsicke, B. T. 2014a, MNRAS, 445, 2244
Veras, D., Shannon, A., & Gänsicke, B. T. 2014b, MNRAS, 445, 4175
Vidal-Madjar, A., Lagrange-Henri, A. M., Feldman, P. D., et al. 1994, A&A, 290, 245
Watanabe, J.-i., Kawakita, H., Furusho, R., & Fujii, M. 2003, ApJL, 585, L159
Weaver, H. A., Feldman, p. D., Festou, M. C., A'Hearn, M. F., & Keller, H. U. 1981, Icar, 47, 449
Weaver, H. A., Feldman, P. D., McPhate, J. B., et al. 1994, ApJ, 422, 374
Wegmann, R., Dennerl, K., & Lisse, C. M. 2004, A&AS, 428, 647
Welsh, B. Y., Craig, N., Crawford, I. A., & Price, R. J. 1998, A&A, 338, 674
Welsh, B. Y., & Montgomery, S. 2013, PASP, 125, 759
Welsh, B. Y., & Montgomery, S. L. 2015, AdAst, 2015, 980323
Welsh, B. Y., & Montgomery, S. L. 2018, MNRAS, 474, 1515
Welsh, B. Y., & Montgomery, S. L. 2019, RNAAS, 3, 25
Wilson, P. A., Kerr, R., Lecavelier des Etangs, A., et al. 2019, A&A, 621, A121
Wilson, P. A., Lecavelier des Etangs, A., Vidal-Madjar, A., et al. 2017, A&A, 599, A75
Wooden, D. H., Ishii, H. A., & Zolensky, M. E. 2017, RSPTA, 375, 20160260
Wyatt, M. C. 2008, ARA&A, 46, 339
Wyatt, M. C., Panić, O., Kennedy, G. M., & Matrà, L. 2015, Ap&SS, 357, 103
Wyatt, M. C., Smith, R., Greaves, J. S., et al. 2007a, ApJ, 658, 569
Wyatt, M. C., Smith, R., Su, K. Y. L., et al. 2007b, ApJ, 663, 365
Wyatt, M. C., van Lieshout, R., Kennedy, G. M., & Boyajian, T. S. 2018, MNRAS, 473, 5286
Wyckoff, S., Tegler, S. C., & Engel, L. 1991, ApJ, 367, 641
Xing, Z., Bodewits, D., Noonan, J., & Bannister, M. T. 2020, ApJL, 893, L48
Xu, S., & Jura, M. 2012, ApJ, 745, 88
Xu, S., Jura, M., Klein, B., Koester, D., & Zuckerman, B. 2013, ApJ, 766, 132
Xu, S., Zuckerman, B., Dufour, P., et al. 2017, ApJL, 836, L7
Ye, Q., Kelley, M. S. P., Bolin, B. T., et al. 2020, AJ, 159, 77
Zhang, Y., & Lin, D. N. C. 2020, NatAs, 0, 77
Zieba, S., Zwintz, K., Kenworthy, M. A., & Kennedy, G. M. 2019, A&A, 625, L13
Zuckerman, B., Koester, D., Melis, C., Hansen, B. M., & Jura, M. 2007, ApJ, 671, 872
Zuckerman, B., Koester, D., Reid, I. N., & Hünsch, M. 2003, ApJ, 596, 477
Zuckerman, B., Melis, C., Klein, B., Koester, D., & Jura, M. 2010, ApJ, 722, 725
Zuckerman, B., & Song, I. 2012, ApJ, 758, 77